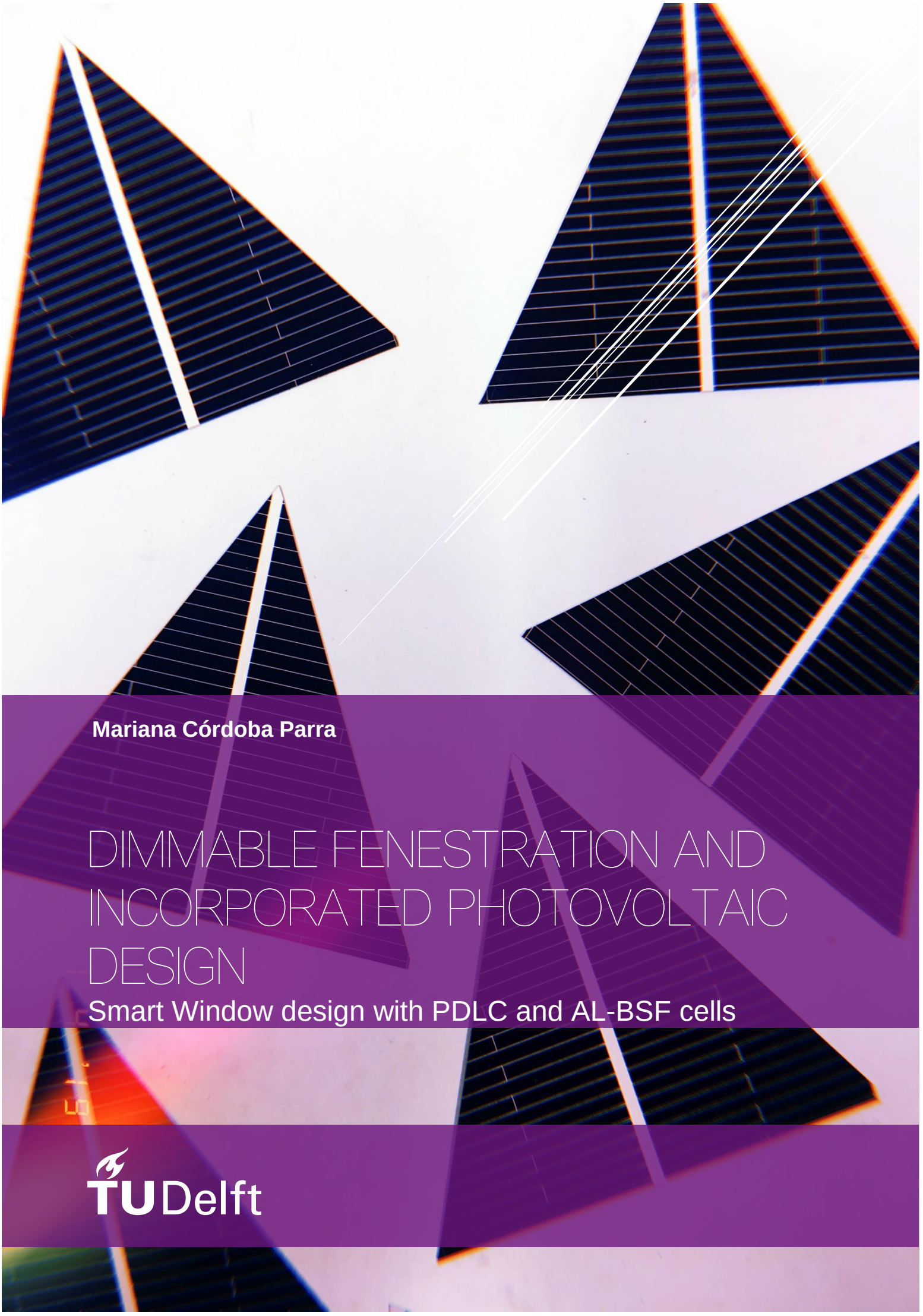

**Mariana Córdoba Parra**

# DIMMABLE FENESTRATION AND INCORPORATED PHOTOVOLTAIC DESIGN

## Smart Window design with PDLC and AL-BSF cells

TU Delft

# DIMMABLE FENESTRATION AND INCORPORATED PHOTOVOLTAIC DESIGN

## Smart window design with PDLC and AL-BSF cells

By

Mariana Córdoba Parra

in partial fulfilment of the requirements for the degree of

**Master of Science**

in Sustainable Energy Technology

at the Delft University of Technology,

to be defended publicly on Friday, 30th of August 2019, at 3:00pm.

| | | |
|---|---|---|
| | Supervisor: | Dr. Olindo Isabella |
| Thesis committee: | Dr. Olindo Isabella, | TU Delft – PVMD Group. |
| | Prof.dr.ir.Miro Zeman, | TU Delft – PVMD Group. |
| | Prof.dr.ir.Tillmann Klein, | TU Delft – Architecture. |

*An electronic version of this thesis is available at http://repository.tudelft.nl/.*

TU Delft

# Preface

*Mariana Córdoba Parra*

*Delft, 12th of April 2019*

The world is reaching a point of no return when it comes to climate change. Humans have been using the natural resources without knowing the consequences of these actions for decades. Since the invention of the steam engine, human race have had a vertiginous technology growth and with it, the exploitation of oil, coal, natural gas and many others. After years of economic growth and new developments, at the end of the 20th century, many scientists and researches warned the international community that the way Earth's resources were being exploited will end up in a climate crisis. This crisis could lead to the extinction of many species including humans.

To solve the crisis, a complete restructuring must be done in every area of human development, from agriculture to nanotechnology manufacturing. In 2015, in a late response from the governments, an agreement between 197 parties was made. This is known as the ***Paris Agreement*** and among its goals, several refer to the build- capacity and technology growth. In general terms it points out that "accelerating, encouraging and enabling innovation is critical for an effective, long-term global response to climate change and promoting economic growth and sustainable development [1]." What this implies is that research has to be supported inside the parties that signed the agreement to achieve a real change. It also states that developing countries will need the support from developed nations in areas of research and new technology development. These technologies should challenge the traditional "unclean" industrial solutions.

One of the areas that has had the greatest spotlight is ***electricity production***. This comes as no surprise, since it is used in every sector. The way humans produce electricity is non-sustainable. The resources used emit gases that increase the greenhouse effect and this changes the climate conditions of the planet, among other things. As a response to the need of clean resources, several technologies to harvest energy have been invented. Wind energy, solar energy, tidal energy and many others now have each their own technologies that convert the power they provide into useful electricity for humans to consume.

Solar energy, in particular has grown from around 75 GW installed capacity in 2016 to 99.1 GW in 2017 making it "the fastest growing power generation source [2]." Research in this area is going strong and the only way to keep the numbers going up is by continuously improving these technologies and also finding new ways to incorporate them in the industry. One of the industries where solar energy has a lot of potential is the ***built environment***.

The built environment represents 36% of the global energy consumption and almost 40% of the $CO_2$ emissions [3], so the urge to decrease these values is huge and there are many ways to do it. In this project you will find that the options are infinite and that creativity and sustainability can go hand in hand. As an engineer it is possible to create appealing and interesting products that can change the approach of more traditional industries, like the construction industry.

As a ***sustainable energy system integrator***, my aim is to make a change and I hope this project serves as a starting point and as an inspiration for many new ideas, designs and implementations of photovoltaics in the built environment.

# Contents

# Abstract

The built environment contributes with 39% of the $CO_2$ emissions in the world [3]. At the same time it is a sector that is expected to grow from US$10.9 trillion (2017) to US$12.9 trillion (2022) [4]. A sector with such an economic growth but with a negative environmental impact needs to innovate in order to reduce its carbon footprint. These are the reasons why, along this project, one of the most traditional components of the building façade will be re-designed. Glazing is a key component for the transformation of the built environment into a cleaner sector. Through glazing, radiation and natural light are received. With smarter window designs that make use of switchable films (films that change their transparency with different impulses) this reception could be done in a more efficient way. This can reduce the need of other artificial devices like air conditioning and light bulbs inside the buildings. Furthermore, if glazing is coupled with solar energy harvesting technologies like solar cells, an autonomous device can be created. A smart window that includes photovoltaic solar cells and an electrically switchable film is prototyped through this project. The selection of materials and construction of the window are explained through this document. Software modelling to recreate real life scenarios during a whole year are performed and the results are encouraging. An off-grid photovoltaic system that supplies energy to an electrically switchable film, all coupled in a glazing for building façade is technically possible, even in challenging environmental conditions.

# Acknowledgements

I understand how serious these projects can be, but in the acknowledgements I want to write in a more informal way. There are two people that made this whole experience possible for me and I don't want to be short on words for them. Leaving my country to come to a whole new continent has been one of the hardest things I have ever done, it has also been the most rewarding. I wouldn't have done any of this if it wasn't for my parents Johanna and Alfredo, who have always been by my side even when physically they are at the other side of the world. These two people have shown me unconditional and selfless love, they have never stopped my dreams and they have always helped me achieve them, and for this I will always be grateful. LOS AMO. I want to thank Juan Camilo Ortiz, because he was the best PhD supervisor I could ask for, he was always willing to help and of course his serenity and great sense of humour made this project absolutely amazing. I want to thank Dr. Olindo Isabella, because since the beginning of the project he was always very clear about what he expected and he always encouraged me to add my personal touch to the project. Finally, I want to thank my friends, all the friends that I have met during this life changing experience. They have been a never-ending source of fun and support, lately more support than anything. Getting to know every culture and the traditions that everyone holds has been one of the most enriching aspects of this master. Thank YOU all for sharing this experience with me.

# List of figures

# List of tables

# 1 Introduction

## 1.1. Project Motivation

Building Integrated Photovoltaics or BIPV is a branch in photovoltaics (PV) research that specializes in including PV materials and devices innovatively in the built environment. The built environment, as it will be discussed later, includes many structures and spaces, which makes the research rich and very broad. For this project, the focus will be on fenestration.

Fenestration refers to “glazed openings [5]” that can be found in buildings, houses, and in general, built structures. This group covers windows, skylights, glazed doors and glazed walls [5]. The interest in fenestration relies in the re-design potential they have and the way they can be used to save energy in the entire building. As it will be shown, saving energy is a decisive move to reach the milestones agreed upon in the Paris accord.

The built environment represents 36% of the global energy consumption and almost 40% of the $CO_2$ emissions [3], so there is an urgent need to decrease these percentages. Changing the current design of fenestration in the envelope of buildings and houses “can together reduce annual energy of a building by 47% [6].” The main reason is that “glazing … [is] responsible for 20-40% of energy used in a building [6]” so making smarter designs that respond to environmental conditions is a promising research area.

## 1.2. Research Questions

1. What are the advantages of PDLC with smart transmittance over other fenestration methods?
2. What is the energy requirement for the implementation of PDLC in built environment and how can PV be coupled to it?
3. What is the feasibility of the final design in a real life case scenario under different shading conditions?

To achieve a fenestration design that aligns with the masters programme objectives, 3 research questions were formulated. The first thing that is important to address is what type of glazing technology, emphasising in the dimmable ones, was better for the overall needs of the built environment. Because this project comes from a line of projects done before, the PDLC was chosen previously. Even though this was the case, it was necessary to revise the reasoning behind this decision and the first question will be answered through this project.

The second question was about the feasibility of having an autonomous dimmable fenestration in the built environment. For this the energy requirement is key, because the objective of the design is for it to be self-sufficient and that there is no need to rely on the building source of energy to operate. Naturally, because of the self-sufficient aspect of the product there has to be a power limit required that can be covered by the PV device. This PV array has to be designed taking into account the restrictions in area, orientation and module angle.

The last question is related to the design itself. The aim is to know if there is a difference regarding the position of the PV array in the fenestration, or of the whole product itself in

the building. This question also addresses the sensitivity of the design to shading in a real case scenario modelled with System Advisor Model (SAM).

## 1.3. Project Overview

To make a smarter design of a fenestration that incorporates photovoltaic technologies, research in materials has to be made. Ideally, the fenestration should be able to become transparent when needed. For example, when there is high irradiation from the sun and it is needed for natural lighting, the window will be able to be switched to a clearer state and permit certain wavelengths. This action will be key to reduce the use of artificial lighting, for example. Many other advantages like this can be drawn from smart fenestrations.

In the case of this project, material research will be done in the area of switchable glazing. This type of glazing is most commonly known as Switchable SHGC (Solar Heat Gain Coefficient) and as it will be explained later in this report. The main feature is that it changes its transmittance when actuated with electricity, a light source or heat, among others.

After the selection of a suitable material for the glazing, a design that incorporates PV technology has to be made. The purpose of the PV in the design is to harvest the necessary energy to change the transmittance of the glazing, meaning that no extra energy from the main grid or main energy source of the building will be used. Because the device is meant for a particular industry, the built environment, it has to be designed in a way that appeals and matches the general characteristics of the industry. This is why aesthetics are taken into account and innovative shapes will be part of the final product. The prototype is going to be designed for the weather conditions of Delft, Netherlands.

In this report, the project will be unravelled. The first chapters talk about the built environment, the relationship it has with sustainability and the concept of Nearly Zero Energy Buildings. After this, an introduction to glazing will lead to the chapter on smart window technologies. This project will emphasize on electrically switchable smart windows, the reason for this will be explained throughout the text. After a comparison of the different window technologies, the selected one will be discussed in a detailed chapter about manufacturing, functioning and the relationship it has with the built environment.

The next chapters will revolve around the other technological components needed to realise the prototype of the smart window, apart from the type of glazing. These chapters will focus on the general description of these technologies and the final selection for the present work. The next section will illustrate the concept design and the ideas that lead to the final concept. It will also explain in detail the different components. The last sections of the report will focus on how the smart window was manufactured. It will also explain how the glazing technology was characterized and the results of this characterization. Finally the report will present the simulation results and the conclusions of the current work. The future projects that need to be done for the prototype to be tested will also be discussed.

# 2 Built Environment

The built environment is an essential part of human development, and as Tom J. Bartuska says in the first chapter of one of his books "the built environment is created to fulfil human purpose [7]." Most of the places humans spend their days and even their lives in are part of the built environment. Now a days, only few inhabitable places on Earth haven't been modified. This last statement should be enough reason to start paying attention to what has been done and how the built environment can be re-designed to be efficient and use ***cleaner*** energy sources. This section will revolve around the relationship between the built environment and sustainability and it will finalize with building façade and glazing.

## 2.1. Sustainability Approach

Sustainability is a concept that has been around since the 1970's when the first issues involving climate and the misuse of natural resources started surfacing. Around this time, the First World Climate conference was held in Geneva in 1979 where sustainability was one of the revolving topics. Sustainability is a concept coined to explain the need to live meeting ones needs but taking into account that in the future other generations should be able to enjoy a healthy and comfortable life style too. This concept relates not only to environmental issues but social, political and economic decisions that will affect future generations [8].

One way to achieve a sustainable way of living, related to energy consumption, which is crucial for human development, is by using sustainable energy technologies. Sustainable energy technology refers to every device used to harvest energy that comes from sources that can't be deployed, i.e. the sun, the wind, the water movement. This technologies are being studied everyday all around the world to improve them and make them as efficient and accessible as possible. This means that in the near future people will be able to enjoy energy coming from sources that will allow new generations to live on Earth.

There are many areas where there can be a disruption from sustainable energy technologies. One of this areas is the built environment, like it was stated by Joseph Sarkis et al:

*"The intergenerational aspect of sustainability is even more pertinent in the built environment since the structures are typically influencing the needs and requirements of future generations* [9]*."*

First, it is necessary to explain in better detail what does built environment mean. "The built environment includes all buildings and living spaces that are created, or modified, by people [9]." This area represents around 0.5% of the available land on Earth [10] but in 2015 represented 36% of the global energy consumption and it has been growing ever since. In other words, even though the built environment appears to represent a small percentage of physical occupancy in the world, it is using one third of the energy consumed and emitting the 39% of the $CO_2$ [3]. These values are shown for this and other industry sectors in Figure 1 and Figure 2. But "built environment" not only encompasses the obvious physical structures and roads, "it also includes the infrastructural elements such as waste management, transportation and utility transmission systems put in place to serve this building space [9]." This would mean that the built environment is a net of different elements that work together to make the space

habitable and it has a bigger carbon footprint than the one accounted for only by the buildings.

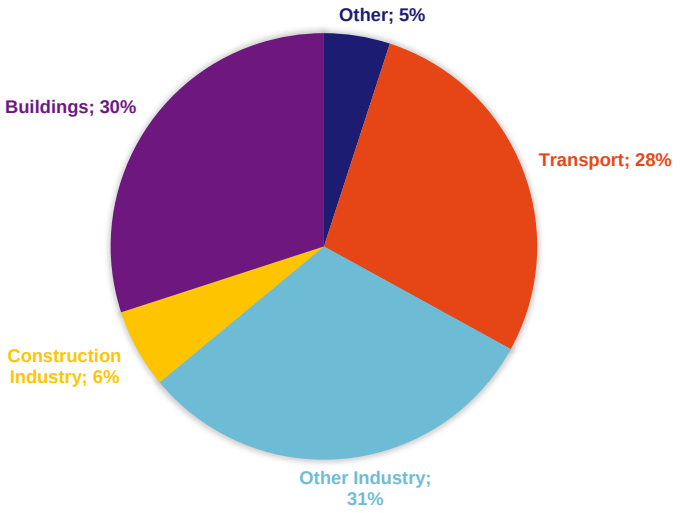


**Figure 1 Share of global final energy consumption by sector. Adapted from [3].**

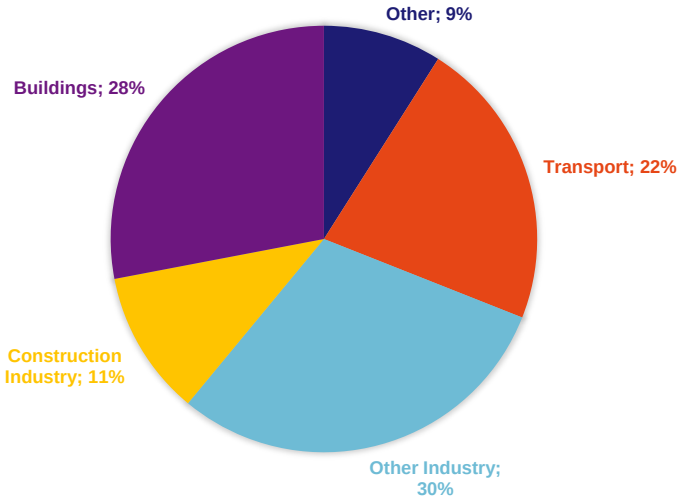


**Figure 2 Share of global energy-related $CO_2$ emissions by sector. Adapted from [3].**

Then, the relationship between sustainability and built environment is necessary and the need of "sustainable construction [as] an emerging field of science that aims at incorporating the general sustainable development concepts into conventional construction practices [9]," is necessary to achieve a reduction in $CO_2$ emissions and make the whole building process more sustainable.

Although until now, the sustainable construction and merging of sustainable technologies in the built environment seems pretty straight forward, "It is important to remember that the built environment is far from homogenous, […] and that the buildings and structures already existing require a variety of approaches [11]."The heterogeneity of the built environment makes it impossible for constructors, architects and engineers to come up with one single solution that fits all. This is why this field is adopting theories and different schemes that can be applied to a variety of scenarios to come up with the best result adjusted for each case. However, this is not the only issue this sector has to face, "It can also be argued that energy used through the constructed environment is driven by the people inhabiting and using buildings [11]," this is why in combination with what has been

already mentioned “significant efforts have [to be] … made to explore and influence human behaviour with regard to sustainable lifestyles [11].”

On the other hand, looking at the bigger picture “buildings exist as part of a wider landscape, rather than in detached isolation [11],” this make it necessary to take into account the surroundings and the harmony of the sector, in the sense of aesthetics and architectural approach. “Therefore, various initiatives have attempted to identify such connectivity, and to explore how emerging technologies can begin to drive sustainable changes [11].”

To show an example of the theories that are being developed or modified to match the built environment, there is one coined in 2009 that derives from Ecological Modernization Theory (EMT) and it is re-named as Sustainability Modernization Theory. This theory originally “puts heavy emphasis upon technological advancement; the invention-innovation-diffusion of new, cleaner technologies and techniques [9]” and it states that “even though the built environment has rarely been integrated into the discourse on EMT, recent efforts have been made by leading countries such as the Netherlands to begin involving this industry [9].” However, what is important from this example is that the theory wants to emphasize in the fact “that innovations (technological, procedural, or process) may be the most effective method to integrate sustainability such that win-win-win opportunities may be maximized [9]” making attractive for the actors of the built environment to invest in research and development (R&D) of new technologies for their specific field. “Thus, ecological modernization at the industry and micro-economic level seeks to identify, evaluate, and implement solutions that will help to advance organizations and the industry in both economic and environmental dimensions [9].”

## 2.2. Controlled Energy Buildings

As it has been said before in this report, “Buildings account for somewhere between 40 and 60 % of energy use across Europe [11],” this implies that in many countries of the European continent, not to say all of them “at a policy level, there have been a series of strategies […] developed to address the possibility of increasing energy scarcity [11].” The previous statement implies that this decisions have “a direct effect on the way in which [people] plan for, design, build and use the built environment [11].”

One of this strategies, different from EMT, is called the Nearly Zero Energy Buildings (nZEB). It was introduced in 2010 by the Energy Performance Buildings Directive (EPBD) and it refers to “a building with very high energy performance where the nearly zero or very low amount of energy required should be extensively covered by renewable sources produced on-site or nearby [12].” The EPBD also set some targets, these were initially: making all public buildings in Europe nZEB by the end of 2018 and converting all buildings by 2020 but “as Europe becomes increasingly urbanised […] the importance of cities and the manner in which they are able to respond to climate change, to some extent dictates whether efficiency targets can be met [11].” It has been proven that meeting these goals is harder than it seems without combining other strategies, such as the creation of new technologies specially designed for the built environment. This last statement was done by Richard Laing and as he says: it is “important to address building standards, and the manner in which they can be used to drive change, including the application of technological solutions including air tightness and the suggested implementation of sustainability labelling [11].”

Some entities have been contributing to the faster adoption of sustainability and nZEB, for example, “the European Construction Technology Platform (ECTP) gave rise directly to the energy efficient buildings initiative, in addition to giving direction to wider European R&D expenditure [11],” and others are creating initiatives to promote the adoption of new technologies like CIC Start with “the ‘Smart Cities’ initiative [11].”

## 2.3. Introduction to Glazing

If new technologies are being adopted and more importantly, embraced by architects, engineers and constructors, these have to adapt to the current façades and the way humans have been designing regular buildings for the past decades. There are several areas in the building construction and design where new technologies could be adopted and some of them need to change faster than others. The reason why there is a more pressing need to find solutions in some particular areas, is because of the amount of energy that is wasted through them.

For example, “a substantial portion of energy consumption by buildings is through its dissipation via building façade [13].” A very important fact about façades is “it has elements that contribute significantly with the heat transfer [14],” making it crucial for the energy exchange between the environment outside of the building and the inside of the structure. There are two factors that are used regarding façade elements: “thermal quantities (e.g., U-value) and solar heat gain quantities (e.g., solar heat gain coefficient (SHGC)) [15].”

The ***Solar Heat Gain Coefficient*** or SHGC is “the fraction of incident solar radiation that enters a room through a glazing in the form of transmitted radiation or secondary heat gains due to the inward flowing fraction of thermal radiation from the window [6].” In other words, it is the coefficient that differentiates the radiation that enters into a room through a glazing in the form of: transmitted radiation, and secondary heat gains.

It is clear that this coefficient applies to the glazing in the façade and this makes the glazing an imperative part of it. From now on, glazing will be the main focus of this project and to start the discussion about it, the different types of glazing according to the SHGC will be discussed briefly.

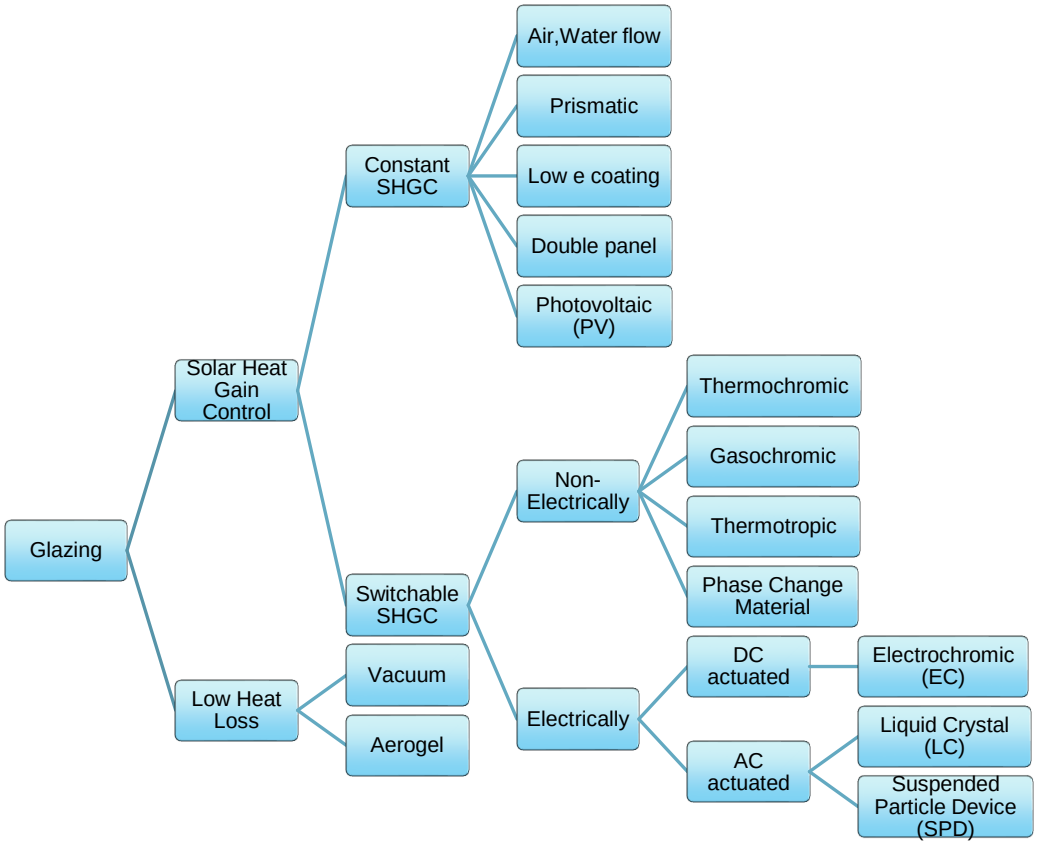


**Figure 3 Glazing division. Adapted from [6]**

In Figure 3, a diagram of the division of glazing with respect to the solar heat gain control and the low heat loss is shown. As it can be seen, the solar heat gain control is much more specified in this diagram, and it is advantageous for the purpose of this project. In the SHGC glazing there are two different options, either a glazing designed to have a switchable SHGC or one with a constant SHGC. In the constant branch we can find common glazing, prismatic, photovoltaic (i.e. semi-transparent amorphous silicon), double panel and some others. In the switchable SHGC, there are 2 categories: electrically switchable and non-electrically switchable. In the non-electrical section, technologies like thermochromic glazing, that becomes opaque with direct sunlight due to the change in temperature, appear.

The type of glazing that this thesis project is based on, belongs to the category of electrically AC actuated technologies and it is known as liquid crystal glazing, more specifically polymer dispersed liquid crystal (PDLC). Nevertheless, before focusing in the PDLC, an overview of the different electrically SHGC switchable glazing technologies is going to be presented. The other 2 technologies that can be seen in the diagram are, suspended particle device (SPD) that also belongs to the AC actuated technologies and the electrochromic (EC) that belongs to the DC actuated technologies.

# 3 Smart Window Technologies

Before going into detail with the different types of electrically SHGC switchable glazing, a brief introduction about what does smart window technologies mean and where do they fit in the whole glazing context will be done.

A smart window “aims to control and regulate solar energy influx [16].” The way to accomplish this can be by using different methods. Smart windows “can change their optical properties reversibly from transparent to opaque when heated and cooled, or when subject to an applied electrical current [16].” Under this description, the switchable SHGC glazing is also known as a smart window. This glazing can regulate the transmitted radiation.

These devices are becoming increasingly popular. The reason behind this is the need to include “sustainable solutions” in the building construction, development and design. Before, smart windows were commonly used in office spaces to separate conference rooms, where important private matters were discussed.

## 3.1. Suspended Particle Device

The Suspended Particle Device (SPD) or “electrophoretic device” was first developed by Polaroid in 1934 [17]. This technology has around 3 to 5 different layers. “The active layer has needle shaped dipole particles (<1 mm long) suspended in an organic fluid or gel [17],” this is the main layer of the device and it is sandwiched between to electrodes. When there is no electricity going through the circuit, the particles are completely random and they scatter the light beams. This state is called the OFF state and it is opaque. When the power source is turned on and there is a difference in voltage between the electrodes, the suspended particles in the fluid align and they decrease the scattering, allowing the transmission of light. Under this condition, the glazing is transparent [17].

Some other characteristics about SPD are that the colour of the glazing can be changed by changing the colour properties of the suspended particles, this has been achieved by Toyota Labs [17]. In Figure 4 an SPD schematic can be seen.

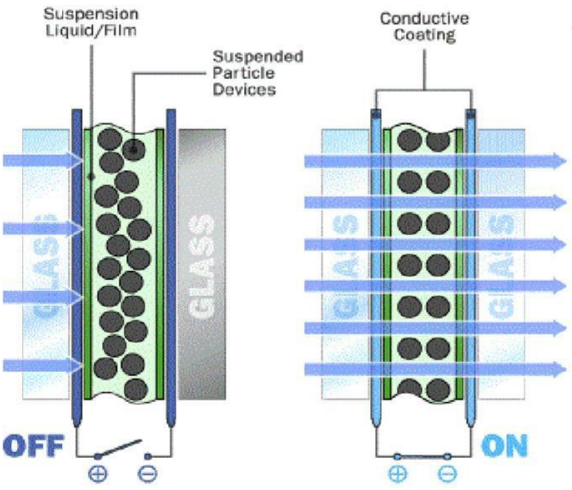


Figure 4 SPD basic working principle schematic. Taken from [18]

## 3.2. Electrochromic Device

First of all, it is important to note that “Electrochromic devices are the most popular technology of large-area switching devices [17].” The main reason of this is their simplicity in general terms. This technology requires low voltages to switch from opaque to transparent and it only needs an impulse and not a constant voltage source to stay in any state [17].

EC has two different categories “transition metal oxides including intercalated compounds, and organic compounds (including polymers) [17].” Each of this categories has a different behaviour that allows the material to change from an opaque state to a transparent state. In the case of inorganic compounds “The […] effect occurs […] by dual injection (cathodic) or ejection (anodic) of ions (Li+) and electrons (e-) [17].” The schematics of the working principle are shown in Figure 5.

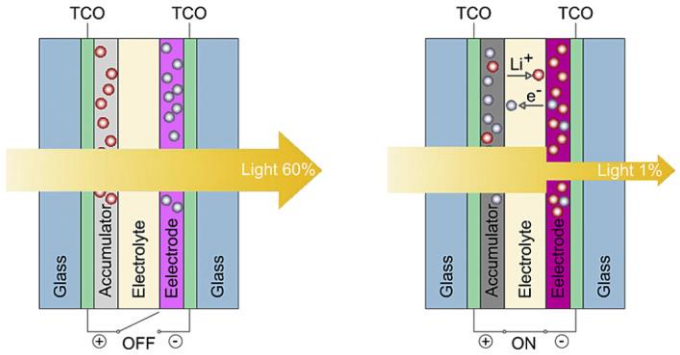


**Figure 5 EC basic working principle schematic. Taken from [19]**

The ions are called coloration ions and they react depending on the voltage impulse sent through the different layers of the EC glass. The amount of layers of an electrochromic glazing can be “from five (or less) layers […] [and they consist] of two transparent conductors, electrolyte or ion conductor, counter electrode, and electrochromic layer [17].” It is important to note that the “ion-containing […] [layer] (electrolyte) [is] in close proximity to the electrochromic layer as well as transparent layers for setting up a distributed electric field [17].” The reason why this is important in the design, is because the engineer wants to distribute diligently back and forth ions into the active layer (electrochromic layer) [17].

## 3.3. Liquid Crystals Device

Liquid Crystal devices have existed since around the 1980’s when the first PDLC (Polymer Dispersed Liquid Crystal) was patented [20]. These devices have been used as both phase modulators and amplitude modulators. The latter group has popular everyday examples like the screens for desktop computers and LCD television [21]. In the area of phase modulation it is possible to find PDLC as a smart glass and PSCT (Polymer-Stabilised Cholesteric Texture) which in simple words is a reversed version of the PDLC [21].

## 3.4. Smart Glass Comparison

In Table 1, a comparison between different characteristics and parameters of the 3 technologies explained previously is done. With this comparison, the aim is to identify the best characteristics of each of the technologies and justify the decision to continue the prototype design with PDLC.

**Table 1 Comparison of different characteristics for the electrically switchable SHGC glazing technologies**

| | SPD | EC | PDLC |
|---|---|---|---|
| Average Direct Transmittance (opaque state) (%) | 20 | 15 | 20 |
| Average Direct Transmittance (transparent state) (%) | 60 | 50 | 80 |
| Voltage Range (V) | 20-150+ | 1-5 | 24-100 |
| Voltage Type (-) | AC | DC | AC |
| Market Status (-) | Young | Mature | Fast Growing |
| Switching time (opaque to transparent) | ~100 ms | 30 s – 2 min | ~100 ms |
| Switching time (transparent to opaque) | ~400 ms | 30 s – 2 min | ~400 ms |

As it can be seen in Table 1, the direct transmittance in opaque state of the EC technology is slightly less than the rest of the technologies, but for business and office application this difference is not relevant. In transparent state, the best direct transmittance is achieved with the PDLC. Better direct transmittance in the transparent state is desired to save energy in artificial lighting. This is even more desirable in a location like Delft, in the Netherlands.

The voltage range is wider with the SPD and PDLC, but lower voltages are required with the EC. In this case, it is more interesting for research purposes to design for higher voltages in a limited area, like glazing. Regarding the market status, the most developed and commercially available technology is the EC, but in the past years the PDLC market has been growing, mainly because of the faster response and better quality of this technology compared to the EC. The switching time is relevant in this case, for user experience a really long switching time will reflect on a higher level of discomfort. To achieve higher levels of comfort the PDLC and the SPD are better technologies than the EC.

Finally, the PDLC has a better outcome than the other 2 technologies in direct transmittance in transparent state, which is the most relevant variable for this project. Also, this technology has the same outcome as SPD in switching time, voltage range and voltage type. SPD has the lowest market status, which will reflect in higher costs and lower availability. These make the PDLC a better option. Even though EC has the best outcomes in voltage range, voltage type and market status, designing for this technology will represent a PV system with a lower complexity in the electrical design and in the area of comfort and aesthetics will not be the most optimal solution.

# 4 Polymer Dispersed Liquid Crystals

A PDLC or a “Polymer-dispersed liquid crystal [,] belongs to a class of electrically, photonically and thermally activated technologies referred to as ‘Smart Glass’ [or ‘Smart Windows’] [20].” This type of composite material presents “both the advantages of a solid polymer and a fluid liquid crystal [22].” PDLC was invented around the 1980’s in the United States of America. In the next few sub-sections the general overview, manufacturing process and relationship of PDLC with the built environment will be discussed.

## 4.1. General Overview

“A PDLC is a two-phase system containing LC domains, usually in the forms of droplets, which are embedded into a polymer matrix [23].” This liquid crystal droplets are in charge of the main functioning of the composite, they “allow controlling […] [the] transmittance by the electrical-driven director reorientation [22].” This means, that when there is a constant electric field going through the PDLC, the LC droplets align and they allow light to pass through the whole film [24]. On the other hand, “In the absence of an electric field [,] LC droplets orient isotropically, scattering [the] incident beam [and] […] becoming white translucent [24].” This reorientation depends on different parameters, some of them are: “droplet size and shape, size distribution, anchoring effects at polymer boundary, liquid crystal dielectric and conductive anisotropy, polymer molecular weight and chemical nature [22].” The schematics of the working principle of PDLC are shown in Figure 6.

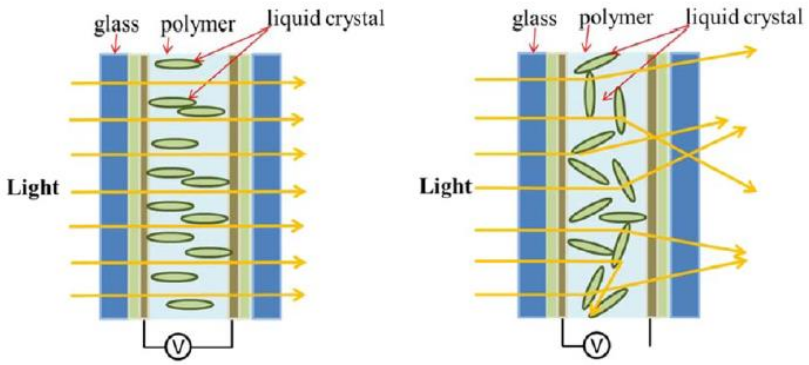


**Figure 6 PDLC basic working principle schematic. Taken from [24]**

In depth, functioning of PDLC can be explained with a refractive index mismatch between the liquid crystals and the polymer matrix they are embedded in. “The index mismatch between the LC and the matrix (nm) causes the parallel beam to refract at the interface, rendering it opaque (off-state),” When an electric field is applied (AC for the case of PDLC), the droplets orientate along the direction of the field. After this, “if the ordinary refractive index of the LC … is equal to that of the matrix … for the incident beam parallel to the electric field, it becomes transparent (on-state) [25].”

## 4.2. Characteristics and Manufacturing

PDLC in a regular version is opaque in the “OFF state”, meaning when there is no voltage difference between the electrodes. In this state, it scatters light because of the refractive

index mismatch. On the other hand, it appears transparent in the “ON state,” when there is an existing voltage difference that aligns the droplets with the matrix.

The reverse operation can also be found, these “devices [are] transparent in their OFF state and opaque in their ON state [22]” and “for safety reasons, reverse mode operation PDLCs […] are preferred in building and automotive applications [22].”

PDLC(s) have an operating voltage “typically […] between 24 and 100V AC [17]” and they are stable “between 0°C and 60°C temperature [6].” The most commonly used electrode for this technology is Indium tin oxide (ITO) [6].

Some of the advantages of this composite, in particular, are that it is “easy to manufacture since their exact thickness is not important; besides they have a low cost [23].” PDLC-based windows also have a “simple structure, durability, fast switching speed, scalability, and mechanical flexibility on flexible substrates [26].” This films also are very good at scattering light in the ranges of 430 to 500 nm (blue and green) when the size of the LC droplets is reduced [6].

Some disadvantages are that “compared to ECs, the power consumption is higher […] because of the need for continuous power in the activated state [17].” Also, PDLC films are very bad at scattering light in the ranges of 600 to 650 nm (red light) [6]. It is also mentioned in several papers that the driving voltages to make the regular PDLC film transparent are high compared to EC. Finally, the response speed to the electrical stimuli could also be improved [23].

The manufacturing process of PDLC is by phase separation and it is an “in situ separation of liquid crystal micro-droplets from a homogenous and refractive index matched mixture of liquid crystal and pre-polymer (or polymer) matrix [27].” For this particular composite there are 3 different techniques that will be explained below.

The first technique is called ***polymerization induced phase separation*** or PIPS, it is considered the most versatile and useful method in present days [27]. In this method a pre-polymer or monomer is needed in the mix with the LC droplets. During the process, the molecules of liquid crystal start forming the droplets and they grow until the polymerization process is finished, this means when the matrix is solid enough and there are no more possibilities to grow. In PIPS, the main factors that affect the size of the LC are: the curing temperature and the type and proportion of the LC in the mix [27].

The second technique is called ***thermally induced phase separation*** or TIPS. The main characteristic of this process is that the polymer has a melting temperature below its decomposition temperature, this implies that it can be melted and mixed with the LC. When the polymer is cooled down to bring it to a solid state again, the LC domain starts growing and it will stop growing when the glass transition temperature of the polymer is achieved. In this method the main things that affect the size of the LC domain are: the cooling rate of the mixture and the component parameters of the LC [27].

The last method is called ***solvent induced phase separation*** or SIPS. In this one both the polymer and the liquid crystal are dissolved in a third agent, a solvent. This solvent doesn’t react with any of the components but it serves as a base to do the mixture. The solvent is evaporated at a certain rate and the LC droplets start growing until the solvent is removed completely. The main factor that affect the droplet size is the rate at which the solvent is removed [27].

## 4.3. Research Status

PDLC as it is, needs improvements in several areas as it can be seen from some of the disadvantages mentioned before. It can also be improved and made “self-adjusting” by using new technologies in combination with this composite. For example, “[PV] technology can be integrated with switchable glass [like PDLC], to give self-powering and possibly wireless features [17].”

In a specific experiment, developed in a university in Italy – *Università della Calabria*- a “Self-adjusting smart window [22]” was done. For achieving this, they proved that “it is possible to combine the electro-optical properties of liquid crystal and the electrochromic properties of electrolyte–liquid crystal mixtures [22]” for the purpose of gaining “control of incident daylight and glare in building and automotive applications [22].” This new approach was obtained by doping with photoconductive molecules a reversed mode operation film [22]. This experiment resulted in a glazing that was highly transparent in the OFF state reaching transmittances larger than 70%. In the ON state it was more opaque at lower voltages when the percentage of photoconductive molecules was higher.

Other improvement was made by the -*Pusan National University*- from South Korea where PDLC was doped with push-pull azobenzene. In this research, part of the problem they wanted to solve, was the thermal relaxation time, which is the time it takes for the PDLC to change from the ON state to the OFF state. This time is longer than the time it takes to change from the OFF state to the ON state because it doesn’t rely on an external source, it only depends on the composition of the PDLC and the natural relaxation of the LC droplets in the matrix. The outcome was that it took less time for the PDLC to change from transparent to opaque than a regular PDLC [28].

One of the most promising improvements was developed by -*Sungkyunkwan University*- from the Republic of Korea in a paper published online in the 26th of June 2018. In their own words “we developed polymer dispersed liquid crystal (PDLC)-based large-area flexible smart windows using continuous roll-to-roll (RTR) slot die-coated Ag nanowire (NW) percolating network electrodes [26].” The purpose of changing the electrode material of the PDLC was to reduce the cost of it when it is done for large-area windows. They also wanted to tackle the brittleness of the original and most commonly used electrode: Indium tin oxide (ITO). The results were 88% average optical transmittance with an applied voltage of 80 V and a cost-effective smart window [26].

Finally some other disadvantages were tackled like yellowing of the film produced by UV aging; and in the way of this, other important parameters of the PDLC were improved. These improvements were accomplished by changing the polymer matrix for a “Glass-gel matrix [25].” The development took place in - *The Sejong University* – in South Korea and the related paper was published in 2017. The main problems the university was tackling were the high driving voltage needed by the film to change the state, the milky haziness in the OFF state and the yellowish colour after some years of being exposed to the UV radiation. The results of this glass dispersed liquid crystal film (GDLC) were even more satisfactory than expected. The response time from the ON state to the OFF state resulted in 3 ms which is “10 times shorter that of conventional PDLC [25].” It also resulted in “low scattering, a clear colourless state, and a low driving voltage [25]” which was the aim.

## 4.4. PDLC and Built Environment

In the past few decades, there has been an increasing concern about the way humans have treated the planet, as it was stated before. Climate change due to the miss-use of fossil fuels among others, has raised some concerns about the conditions living beings will have to face in the future and if these conditions will eventually end some forms of life that inhabit the planet. One of the areas where there can be a change to diminish and eventually erase the carbon footprint is that of the built environment. Even though there are several sub-systems in the built environment, the aim of this work is in the glazing of the façade. It is good to know that one way to tackle the energy efficiency in built environment is by introducing "highly advanced low heat loss, heat gain and comfortable daylight allowing glazing [6]." Taking this into account, the fenestration for built environment also needs to be done in a way that is aesthetically appealing for the market.

To reduce the amount of energy that is used in the built environment and re-design the energy consumption scheme of it, the first step is to know how the energy is used and how much it represents from the global energy consumption. In the built environment "energy [is] used to more generally ensure comfort conditions and artificial lighting head to buildings thus consuming 40% of global energy to meet heating, cooling and lighting energy demands, though this varies in different countries [6]." Specifically, in countries like the US, the energy consumption is 41% from the global energy consumption as well as in the European Union (EU). In china for example, it is about half of this value and in places like Japan is 14.2% which is almost a quarter from the consumption of EU. In all cases the consumption has heavily increased compared to a few decades ago [6]. In particular, "Glazing are responsible for 20-40% of energy used in a building [6]." In this way, "insulation and retrofitting lower heat loss glazing can together reduce annual energy of a building by 47% [6]."

Focusing on fenestration for the building façade means that the design developed here can have different uses in a building and will not only be thought of as a regular window. To start the overview, smart windows and the different novelties surrounding them will be refreshed. "Smart windows are used in building and automotive applications in order to control the incident daylight and glare according to occupant comfort [22]," and to make it smart and also autonomous "photovoltaics can be integrated as power sources […]. In this way a switchable window could be a completely stand-alone smart system [17]." Making key components in buildings autonomous gives several advantages, some of them are: a more reliable performance, also the automatic reaction of the device makes it easier for the user to concentrate in other activities without prejudicing the electricity consumption, and finally avoiding the usage of electricity from the main grid because the device is capable of self-sufficiency in terms of energy use [6].

In the area of PDLC-based switchable windows, they "are best suitable over other types for glazing as [...] [they do] not require polarizer to operate, [and they have] high brightness (because of its high transparency) [26]." They also have a fast response, there is no need to treat the surface of the material, they have a wide view angle and because it needs a constant power source different levels of opacity can be achieved by tuning the voltage [26]. Another important advantage of PDLC is that is "generally intended to… [be used] for large scale glazing application ($1m^2$) [6]" which means that there is less restriction in how it can be used in the design of modern buildings. Matching this technology with PV technologies "enables fossil fuel generated electricity free glazing actuation, which trigger to modulate from opaque to transparent state or reverse depending upon indoor and outdoor ambient conditions [6],"and it serves as an advantage for energy savings in the built environment.

# 5 Technology Overview

This section will revolve around the components needed to build the autonomous smart window, asides from the PDLC that was discussed in chapter 4. For the solar cell technologies, only crystalline silicon is being discussed because it is the most mature and readily available technology in the industry right now. The electronic components commonly known as the ***balance of system***, will be also explained.

## 5.1. Solar Cell Technologies

Crystalline silicon (c-Si) solar cells are "the working horse of the PV energy market […] [since their] invention in the 1950s up to today [29]." They are called crystalline because the lattice is in a pattern that repeats itself [30]. There are 2 types of surface in c-Si, one is called the 100 surface and the other one is called the 111 surface. The first one is a diamond cubic crystal structure and each silicon atom here has 2 valence electrons. The 111 surface has a pyramidal structure and each silicon atom has 1 valence atom [30].

There are 2 types of crystalline silicon, depending on the defect density of the bulk: monocrystalline and multicrystalline, also called polycrystalline. Monocrystalline silicon has a lattice that is "continuous and unbroken [30]." One of the most important aspects of this type of silicon is that with "no grain boundary, much larger open circuit voltages can be obtained [30]" and this implies that it can be used in high efficiency solar cell designs. The polycrystalline type of silicon on the other hand has many grains and between them, grain boundaries can be found. This grain boundaries represent lattice mismatches or defects and this is why charge carrier lifetime is shorter in polycrystalline than in monocrystalline silicon [30].

The common c-Si solar cell also known as ***Al-BSF solar cell*** is the first type being considered for this design. This traditional cell gets the name from the concept of Back Surface Field which is a solution for recombination at the back metal-semiconductor interface. A Back Surface Field (BSF) is a "highly doped p-region that is placed above the point contacts [30]." The objective of BSF is to reduce the contact resistance and the recombination velocity at the rear of the cell. For this project the cells available have the characteristics, shown in Table 2.

**Table 2 Al-BSF Cell Characteristics under STC [31]**

| Characteristics | Values |
|---|---|
| Efficiency Code | ETS6-2060 |
| Size (mm) | 156.75 x 156.75 |
| Efficiency (%) | 20.60 |
| Maximum power point current (A) | 9.09 |
| Maximum power point voltage (V) | 0.55 |
| Short circuit current (A) | 9.63 |
| Open circuit voltage (V) | 0.66 |

The second type being considered, is a high efficiency concept that was introduced to the market by Sunpower. This concept is known as ***Interdigitated Back Contact*** (IBC) solar cell. The 2 advantages of this solar cell are that the wafer is done with n-type silicon which in comparison to the traditional p-type wafer doesn't suffer from light induced degradation. The second advantage is related to the collection of the charge carriers, both of them are collected at the back. This means, the front of the cell is metal free, so the shading component from the metal connections is absent [30]. The characteristics of

this solar cell are shown in Table 3 and in Figure 7 the front and back view of the solar cell is shown.

Table 3 IBC Cell Characteristics under STC [32]

| Characteristics | Values |
|---|---|
| Name | Ultra Peak Performance |
| Size (mm) | 125 x 125 |
| Efficiency (%) | 24.3 |
| Maximum power point current (A) | 5.89 |
| Maximum power point voltage (V) | 0.63 |
| Short circuit current (A) | 6.18 |
| Open circuit voltage (V) | 0.73 |

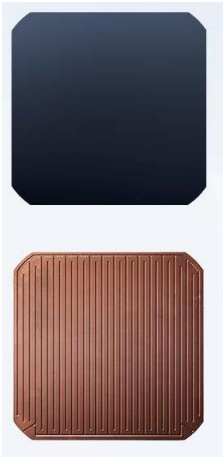

Figure 7 Image of an IBC solar cell front view and back view. Taken from [33]

## 5.2. Electronic Components

A PV system can't be complete without the electric circuit to eventually supply energy to the load. The purpose of a PV system is to generate and supply energy, and the collection of charge carriers is only the first step. Then it is necessary to make a path for the carriers to energize the load or to reach a storage device for future energy needs. This path is composed by several electric/electronic elements that regulate the current and voltage of the carriers.

It is necessary to have regulating components through the connection between the source and the load because this energy flow is not compatible with most of the appliances that PV systems are being used for. The first mismatch is the type of current, PV cells generate Direct Currents (DC) and most of the devices used now a day's work with Alternate Current (AC). Taking this into account, the main component of the balance of system is the inverter. The inverter for this project will be defined as the electronic device that transforms DC into AC [30].

Aside from an inverter, sometimes a DC-DC converter is needed. This type of electronic technology is used to step up or down the voltage produced by the PV array. The boost converter (step-up) is more common when the PV array has small dimensions or it is located in areas where irradiation is low. It can also happen that the load requires a determined higher value of voltage. The contrary goes for the buck converter (step down), when the output of the PV array is slightly high for the application, a DC-DC conversion that lowers the value of the voltage is possible too [30].

Another important software that was created exclusively for PV system electronics is the Maximum Power Point (MPP) tracking. The Maximum Power Point is a specific condition in which a PV device delivers the maximum power possible under the weather conditions that it is immersed in at the moment. This point is easily identified in the current vs voltage curves, known as I-V curves. The point is a global maximum in the instant I-V curve of the PV device. The algorithm that can find this point, can either be pre-programmed and function a fixed way or it can rely on instant inputs measured in the actual system and change depending on these. The first method is called indirect and the second is known as direct. Either of this can be used and it is available in the market, but it is important to point out that it is not a physical component, it comes integrated in DC-DC converters or charge controllers, which will be discussed below [30].

Charge controllers are only needed when batteries are part of the PV system design. Frequently, batteries are included when the system is designed as ***stand-alone*** but it is not exclusive of these systems***.*** This kind of system differs from ***grid-connected*** in mainly, as the name indicates, the grid connection. Charge controllers are necessary to elongate the lifetime of the batteries. If a battery is over-charged and/or over-discharged the lifetime is prejudiced, this is why a control over the amount of current and the range of voltages allowed has to be strictly done.

The last component that has to be taken into account for the design is the cables. Even though it sounds like an easy task, bad design of cabling can result in events that can harm the people involved in the project. For each type of connection a different colour and thickness is needed. The resistance of the cable can be optimized by considering its length and its thickness. In Europe a colour code is used for AC wiring and regarding DC wiring the universal standard, black for negative and red for positive, will be used [30].

# 6 Technology Selection

This section will be about the technology selected for the final prototype and the decisions that had to be made to build each part of the smart window. In many cases there was a need to be creative and to add certain complexity to the final solution. Furthermore, the characterization methods, for some of the technologies, will be presented.

## 6.1. Smart Glass

The first step for selecting the PDLC film is checking the availability of the technology in the market. At the beginning, it seemed interesting to work with the reverse operation PDLC that was explained in section 4.2, but it is not available yet. So after an extensive research and quote gathering, the PDLC was obtained from the company Innoglass. This company specializes in smart films and it is established in China. The two main reasons for the selection of this particular film were the competitive price in the market and the low AC voltage needed (48V) to change the state of the film. The company offers two types of film: the self-adhesive and the non-adhesive. The first one is easier to install and it is aimed for customers that want to change the window system themselves without the need of changing the glass. The later one is aimed for construction and glazing design because lamination under specific conditions is needed. For the project, the two types were acquired. The characteristics of this PDLC, obtained from the datasheet, can be seen in Table 4.

**Table 4 Datasheet Characteristics of the PDLC film [34]**

| | Switchable PDLC film – Milky White |
|---|---|
| Operation Model | Power On: Transparent |
| | Power Off: Opaque |
| Direct Transmittance (Power On) | 79% |
| Direct Transmittance (Power Off) | 4% |
| Haze (ON State) | 4-5% |
| Thickness (mm) | 0.36 |
| Switch Time (ms) | Off to On: 200 |
| | On to Off: 600 |
| Operation Voltage (V AC) | 48 ± 5 |
| Power Consumption ($W/m^2$) | 3.7 |
| Operating Temperature (°C) | 20 to 60 |

As it can be seen in Table 4, the transmittance characteristics of this PDLC are under the common ranges found in literature. Furthermore the power consumption is around 3.7 $\frac{W}{m^2}$, which is ideal for the design of the smart window because it can be achieved with a well-designed PV system without compromising much area of the glazing. For these prototypes the minimum expected voltage from the PV array is around 5 V. The reason for this minimum voltage has to do with the electronic components of the system. These components start working with input voltages around 3-4V so there is a minimum voltage that has to be delivered in ordered to have working prototypes.

Even though most of the information needed could be obtained from the datasheet, the reflectance is also needed to make a complete optical characterization of the film. This information will be used to understand the behaviour of the whole smart glazing system, meaning, when the PV system is assembled. This is the reason why measurements of

transmittance and reflectance were made in the laboratories of the Photovoltaic Materials and Devices (PVMD) department.

The device used for making the measurements was the **LAMBDA 950 UV-Vis Spectrophotometer Perkin Elmer**, it can be seen in Figure 8. The spectrophotometer is used to do optical measurements over different samples. It consists of two main chambers and it has some extra chambers that can be exchanged in order to do different type of measurements. For the case of the reflectance and transmittance of the self-adhesive and non-adhesive PDLC, the chamber used was the Integrating Sphere. This chamber consists of a cylindrical compartment whose walls are covered with Spectralon. Spectralon "is a solid thermoplastic that exhibits the highest diffuse reflectance of any material or coating in the 250-2500nm band" [35].

**Figure 8 LAMBA 950 UV-Vis Spectrophotometer Perkin Elmer. Taken from [36]**

For the transmittance measurements, the sample is located at the entrance of the compartment, where the beam is going to pass. When the light beam crosses the sample, the Spectralon reflects the light and it is read by the two measuring devices that are inside the cavity. One measuring device covers the range from 175 nm to 860 nm and the other one from 860 to 3300 nm. This configuration measures the total transmittance. The case for measuring the diffuse transmittance is achieved by opening a "window" inside the cavity that is directly in front of the sample. By doing this, the direct component of the transmittance exits the chamber and the devices measure the diffuse component. In Figure 9 the set-up for transmittance can be seen.

**Figure 9 Transmittance set-up of the PDLC sample in the LAMBDA 950**

The reflectance is done by positioning the sample in the window at the opposite side of the main entrance cavity. This way the light beam that enters the compartment is reflected on the sample and the total reflectance is measured. For the diffuse reflectance a little window opposite to the sample is opened and the direct reflectance component leaves the chamber. The whole compartment has a small angle between the main

entrance of the light beam and the location of the sample. This angle ensures that the direct component reflected by the sample will not interfere with the original light beam and the measurements are trustworthy. The set-up for reflectance can be seen in Figure 10.

Figure 10 Reflectance set-up of the PDLC sample in the LAMBDA 950

## 6.2. Solar Cells

After discussing the types of solar cells that were considered for this design in the previous chapter, quick calculations were done on how many solar cells could be fitted in a prototype of 60 x 60 cm. This dimension constraint is imposed by the laminator available in the laboratories of PVMD of TU Delft, where the prototype is going to be manufactured.

For the IBC cells only 4 cells can fit the window. These 4 cells would be located at the bottom of the window prototype and their voltage output under Standard Test Conditions (STC) would be 2.528 V, which is half of the expected voltage explained in section 6.1. For the Al-BSF cells, the outcome is not better. Only 3 cells can fit the window. The dimensions of the cells can be seen in Table 2. The sketch of this first approach is shown in Figure 11. If only this 3 cells are considered and they are connected in series, the STC output will be around 1.647 V which is underneath the expected voltage. Clearly, under the weather conditions in Delft, the power output will not be enough to power the PDLC when desired most of the year.

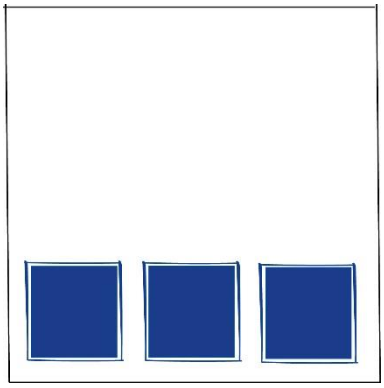

Figure 11 Sketch glass (60x60cm) with 3 AL-BSF solar cells

To solve this problem a new approach on the solar cell design had to be made. The ***design of mini-modules*** is part of the research done by the PVMD group and it matches in many aspects the final purpose of this project. For example, different shapes can be

made in order to have a more appealing product for the building industry and using these, voltages around 10 – 12 V can be reached. As a final decision, incorporating mini modules into the prototype was what fitted best.

The mini modules were designed and hand-made in TU Delft. The manufacturing process will be discussed in detail in chapter 9. In this section, the characteristics of the concept design will be discussed and how the mini modules were characterized in order to obtain their performance values.

After the shape cutting of the original solar cell, each individual mini solar cell has to be characterized. It has to be characterized in order to see if there is a significant current restriction made by any of them. This can happen when all of the mini cells are connected in series and one of them has a significantly lower short circuit current. To obtain short circuit current, open circuit voltage, fill factor, maximum power point voltage and current of each individual cell the laboratory set-up known as WACOM is used. First, "the main parameters that are used to characterize the performance of solar cells [30]" will be explained briefly and then the set-up will be described.

Short circuit current refers to a current measured "when the electrodes of the solar cell are short circuited [30]." This current relies on the incident photon flux and for the case of STC, this flux is determined by the AM1.5 spectrum. Open circuit voltage refers to "the voltage at which no current flows through the external circuit [30]." This corresponds to the highest voltage that can be delivered by a solar cell, it is also called forward bias voltage [30].The fill factor is a ratio, which is also presented as a percentage. This ratio is obtained between the maximum power the solar cell can deliver and the product of the short circuit current, open circuit voltage and the area of the cell [30]. The maximum power in watts can be obtained by multiplying maximum power point voltage and maximum power point current. As it was explained in section 5.2 about electronic components, the maximum power point refers to the optimal operation point of a PV device.

The set-up used to characterize the solar cells is known as ***WACOM***. It is an *AAA* class LED solar simulator. This class tag, means it is one of the best in the market. It replicates the solar spectrum with high precision and it is designed for research purposes. It covers a range of wavelengths from ultraviolet (365 nm) to infrared (1070 nm). It consist of a series of LED lights that can be adjusted through the software to match the requirements of the test [37]. It has a platform were the PV device is located. The set-up can be seen in Figure 12 and a closer look to the platform is shown in Figure 13.

Figure 12 WACOM complete set-up

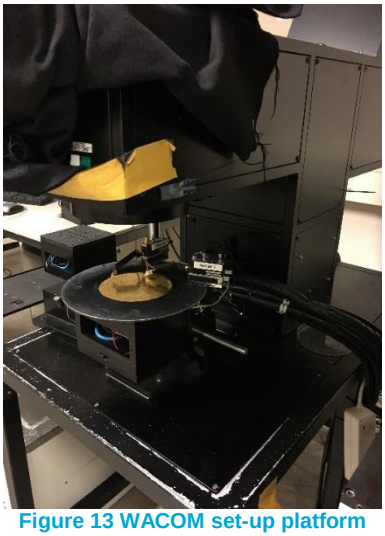

Figure 13 WACOM set-up platform

To perform the measurements, the solar cell has to be connected to the negative and positive cables available in the platform. This is a circuit that is connected to the WACOM and measures all the variables stated before through it. After the cell is located in the platform, the spectrum is configured in the software. In this set-up, an AM1.5 spectrum was used; the solar cells are characterized under STC. When the parameters are adjusted the Wacom illuminates the cell long enough to construct the curve with the amount of points required by the user. The software delivers a file with data points of voltage and current, and the main parameters. The I-V curve obtained from this procedure on a batch of 5 solar cells is shown in Figure 14.

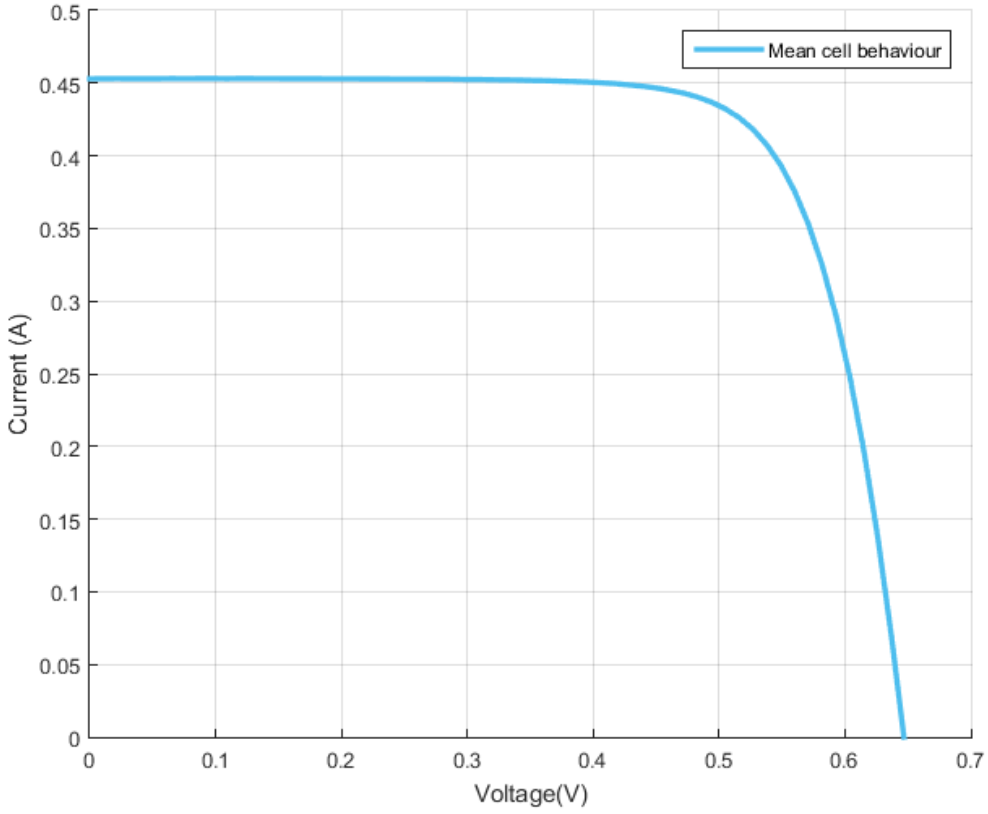


**Figure 14 mean I-V curve of 5 solar cells measured under STC.**

The I-V curve shown in Figure 14 is the result of the measurement of 5 solar cell I-V curves under STC. From these results the characteristic voltages and currents can be known. This values are presented in Table 5.

**Table 5 Average characteristics of the solar cells used in the mini module design under STC.**

| Parameters | Values |
|---|---|
| Short circuit current (A) | 0.45 |
| Open circuit voltage (V) | 0.65 |
| Maximum power point current (A) | 0.43 |
| Maximum power point voltage (V) | 0.52 |

After the solar cells are welded together to form the mini module, an ***electroluminescence*** test is done. The reason to do an electroluminescence test *before* the mini module is laminated is to see in what areas the solar cells are more likely to break, in case they do, when they are laminated. Meaning, another electroluminescence test has to be done *after* lamination. Because of the artisan and experimental nature of

the project this type of analysis have to be done in order to understand which mini module configuration and connection is more viable for constructing the prototype. The viability, for this particular prototype, is determined by the capability of having a uniform energy production where all the modules have around the same parameters.

An electroluminescence phenomenon is “an optical and electrical phenomenon in which a material emits light in response to the passage of an electric current or to a strong electric field [38].” This phenomenon is used in the advantage of the researchers to capture cracks, defects or dead zones in the mini module design. The set-up consists of a high resolution camera located in a tripod, a DC power source, the software for processing the images and an infrared (IR) light source. In the PVMD department the software used is Camera Control Pro 2.

The mini module without lamination is located over a table and connected to the power source. To adjust the current and voltage supplied by the source, the measurements done to the individual cells in the WACOM have to be taken into account. After the set-up is done, the camera and the IR light are turned on. In the computer, the software is initialized and the focus of the camera is adjusted through it. If it is necessary, the camera is moved manually until the complete shot area is right. When the focus and the location of the mini module are correct, the IR light is turned off. The set-up is located in a dark room, this is necessary in order to capture the phenomenon and all the details of the cells. After the dark room is fully closed, a picture is taken through the software. Many pictures can be captured, and they can be checked instantly in the computer in the case any adjustments have to be made. The set-up for the electroluminescence can be seen in Figure 15 and the command computer with the power supply can be seen in Figure 16.

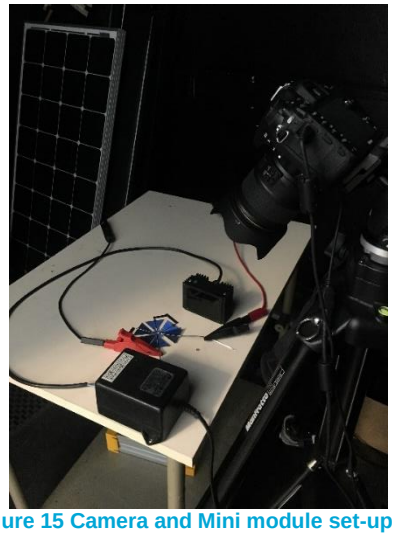

**Figure 15 Camera and Mini module set-up for electroluminescence**

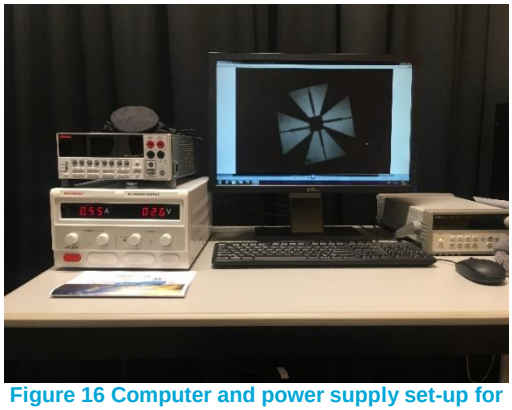

**Figure 16 Computer and power supply set-up for electroluminescence**

Both the WACOM and the electroluminescence procedure have to be done one more time after the mini module is laminated. The WACOM procedure is needed to get the parameters of the full PV mini module. Both procedures have exactly the same steps stated previously.

## 6.3. Electric Circuit

The electric circuit for the design of the prototypes was done based on the circuit used by Yuan Gao in his PhD thesis project called *Photovoltaic Windows: theories, devices and applications* [39]. For one of his multiple projects, Yuan Gao used an inverter to

change the transparency of a scale house model glazing PDLC. The inverter was obtained from the commercial site Smart Tint. The characteristics of the inverter are shown in Table 6.

**Table 6 Characteristics of the inverter used for the prototypes [40].**

| | Values |
|---|---|
| Input Voltage (V-DC) | 12 |
| Output Voltage (V-AC) | 60 |
| Maximum Input Current (A) | 16 |
| Maximum Output Current (A) | 5 |
| No Load Current (mA) | 25 |
| Efficiency (%) | 90 |
| Operating Temperature (°C) | - 40 to +85 |

In Table 6, the main electric characteristics of the inverter used for this project are shown. Even though an inverter with a controllable output voltage was desired, this was not possible because of availability issues with the manufacturer. The PDLC selected works with 48V AC but if a higher voltage is input the transmittance increases. This phenomenon happens due to the material interaction properties of the film.

Asides from the inverter, a charge controller with MPPT is needed. In this case, the selected one was obtained from Hi IC store through Ali Express. The characteristics of the charge controller are shown in Table 7. The characteristics of the MPPT integrated to the charge controller are shown in Table 8.

**Table 7 Characteristics of the charge controller used for the prototypes [41].**

| | Values |
|---|---|
| Nominal Voltage (V) | 18 |
| Maximum Charging Current (A) | 2 |
| Optimal Type of Batteries (-) | $LiFePO_4$ |
| Optimal Number of Batteries (-) | 7 (s) |
| Module Solar Controller Ref | CN3306 |

**Table 8 Characteristics of the integrated MPPT used for the prototypes [42].**

| | Values |
|---|---|
| Input Voltage Range (V) | 4.5 - 32 |
| Operating Temperature (°C) | - 40 to +85 |
| MPPT Pin's Voltage (V) | 1.205 |
| Operating Current Range (µA) | 700 - 950 |
| Efficiency (%) | 81% |

In Table 8, some of the electric characteristics of the MPPT are shown. The value of efficiency was obtained from the PhD thesis figure of Yannick Verbelen from the University of Bristol. The graph used is shown in Figure 17. As it can be seen, 2 different sets of lines are plotted. The short set to the left corresponds to the MPPT CN3065. The lines that cover a voltage range from 4.5 V to 32 V correspond to the MPPT CN3306, which is the one used in this project. For the input voltage of the first prototype which is around 8 V and a unit battery voltage of 3.2 V that can be approximated to be between the blue and yellow dotted lines, an efficiency of 80 to 81% can be assumed.

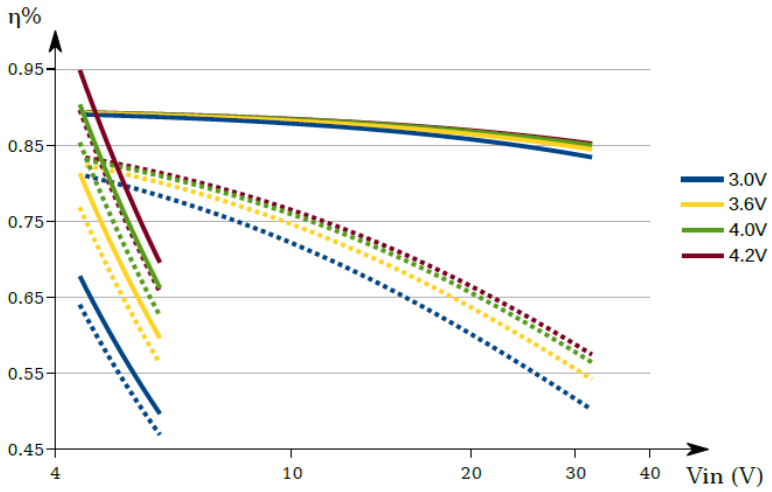


**Figure 17 "Charge efficiency comparison between the linear CN3065 (left steep curves) and switched mode CN3306 battery chargers. Solid curves show a charge current of 100 mA, dotted curves a charge current of 10 mA [43]." Taken from [43]**

Finally the batteries for the project are from Duracell and are specially made for solar applications. These batteries have a chemical composition of lithium and iron and they are most commonly known as $LiFePO_4$. The characteristics of these batteries can be seen in Table 9.

**Table 9 Characteristics of the batteries used for the prototypes [44].**

| | Values |
|---|---|
| Capacity (mAh) | 400 |
| Voltage (V) | 3.2 |
| Energy Density (Wh/kg) | 75.29 |
| Maximum Charging Current (A) | 0.4 |
| Maximum Discharging Current (A) | 0.8 |

With all the components explained in this section, the complete electric system of the project can be sketched. The schematics of the final PV system circuit are shown in Figure 18.

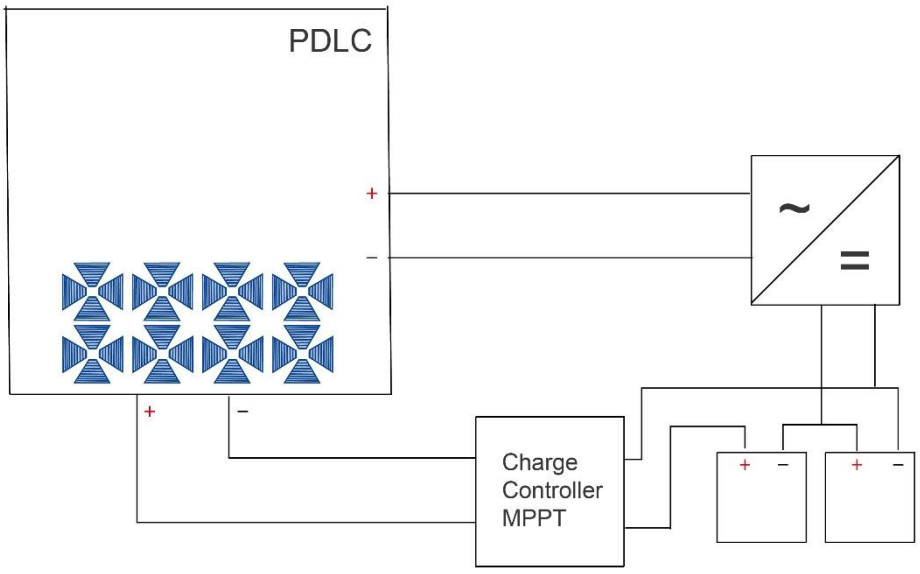


**Figure 18 PV + PDLC system schematics**

# 7 Concept Design

In this chapter the process of designing the two final smart window prototypes is going to be discussed. It will start with some of the basic ideas discussed during the project meetings and it will explain the evolution until reaching the two final prototypes.

The first 2 ideas were based on triangular solar cells and another on hexagonal solar cells. These are shown in Figure 19, Figure 20 and Figure 21, respectively. These were also designed taking into account their basic electronic characteristics, because there are expectations that have to be accomplished in terms of energy generation. The energy generated by the array has to be enough to supply the PDLC and the balance of system. The expected output parameters of these arrays is shown in Table 10.

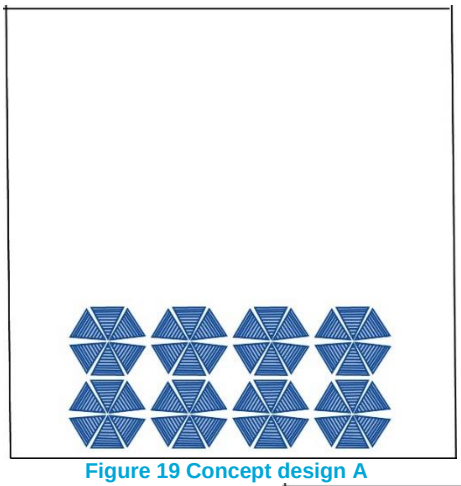

Figure 19 Concept design A

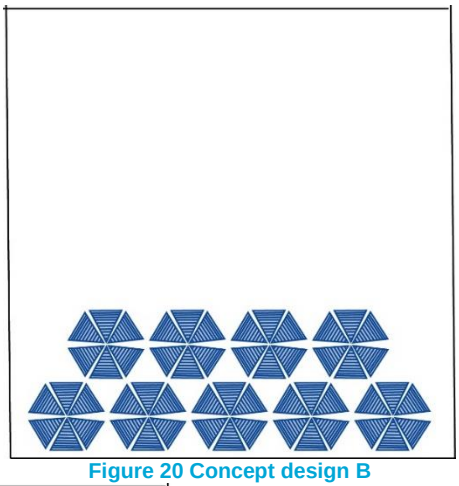

Figure 20 Concept design B

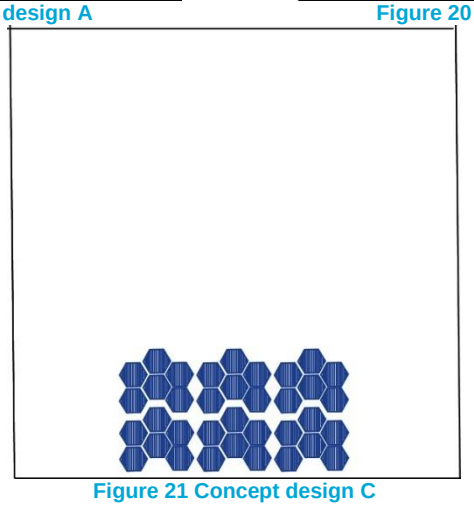

Figure 21 Concept design C

As it can be seen from the figures presented previously, until this point the design was made without any manufacturing restriction. The designs were based on solar cells that were cut in the PVMD mini module manufacturing laboratory without any welding or lamination process done on them. When the whole production process was done for these different shapes, some changes had to be made. In section 8.2, the whole mini module selection process will be explained in detail. What can be said right now is that one of the main reasons to change from triangle shaped cells to trapezoid shape was the fragility of the top corners.

Table 10 Basic characteristics of the first 3 concept designs.

| | Concept A | Concept B | Concept C |
|---|---|---|---|
| Open circuit voltage (V) | 15.36 | 11.52 | 11.52 |
| Short circuit current (A) | 0.64 | 0.95 | 0.64 |
| Connection | 4 mini modules in series - 2 arrays in parallel | 3 mini modules in series - 3 arrays in parallel | 3 mini modules in series - 2 arrays in parallel |
| **Mini Module characteristics** | | | |
| Open circuit voltage (V) | 3.84 | | |
| Short circuit current (A) | 0.32 | | |

When comparing the concept designs shown in Figure 19 and Figure 22, the number of cells per mini module is reduced. This has to do with the information provided in Table 10. The maximum current that can be achieved with concept B is 0.9 A and the amount of solar cells needed for this is 45. If the solar cell is being re-designed to be a trapezoid the current will be reduced because the area will be reduced, assuming the same triangle. To avoid needing more cells, bigger cells were the way to go. This way the design could have less amount of cells. For the first prototype 32 cells were needed and for the second prototype shown in Figure 23, only 24 cells were used. The expected electric behaviour of these final concept designs is shown in Table 11.

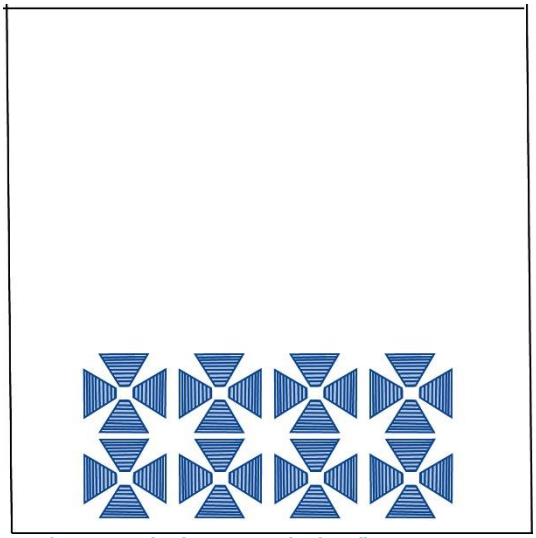

Figure 22 Final concept design first prototype

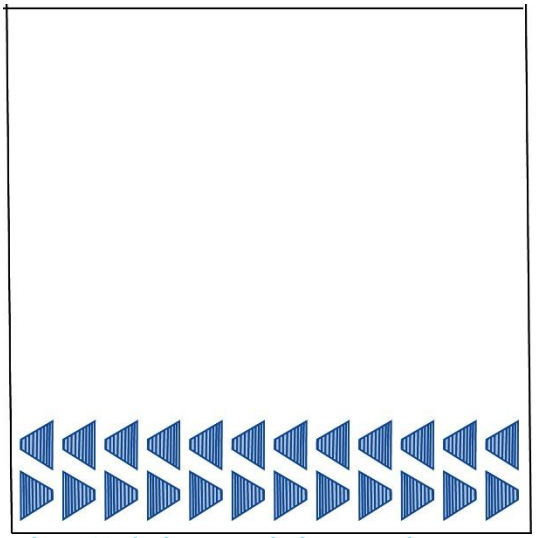

Figure 23 Final concept design second prototype

Table 11 Basic characteristics of the final concept designs

| | First Prototype | Second Prototype |
|---|---|---|
| Open circuit voltage (V) | 10.34 | 7.76 |
| Short circuit current (A) | 0.91 | 0.91 |
| Connection | 4 mini modules in series - 2 arrays in parallel | 12 solar cells in series – 2 arrays in parallel |
| **Solar Cell Characteristics** | | |
| Open circuit voltage (V) | 0.65 | |
| Short circuit current (A) | 0.45 | |

# 8 Characterization Results

## 8.1. PDLC

After performing the measurements of reflectance and transmittance on the PDLC in the OFF state it is necessary to work with the data. With these data it was possible to obtain a complete optical characterization. This characterization included absorption, haze and other variables relevant for the design of a glazing in the built environment.

As it was explained in section 6.1, the procedure for characterization was done in the LAMBDA and the results will be explained with Figure 24, Figure 25 and Table 12.

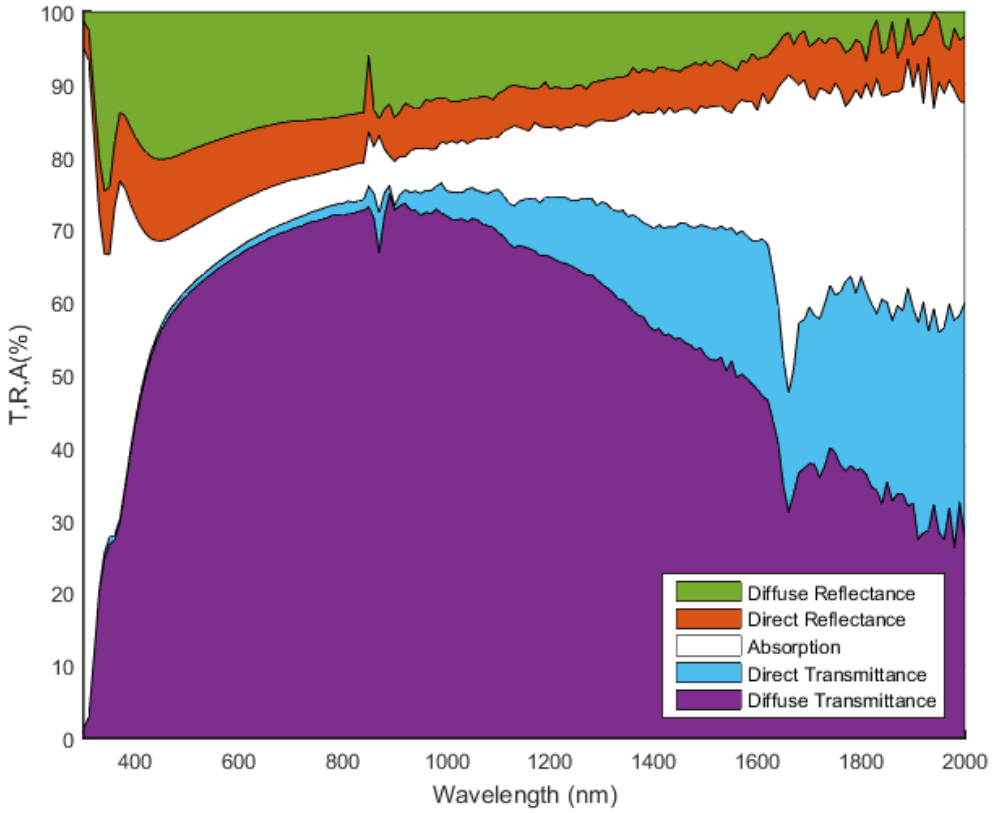


**Figure 24 Transmission, Absorption and Reflectance of non-adhesive PDLC.**

In Figure 24, the behaviour of the non-adhesive PDLC sheet is shown for the range of 300 to 2000 nm. The non-adhesive PDLC refers to the sheet that has to be laminated with the glass in order to be able to install it. The first thing that is noticed from this graph, is the high transmittance of the PDLC, but most of it is in the form of diffuse transmittance. For the visible light range (380-750 nm) the average value of diffuse transmittance is 61.99%. For the case of reflectance it is mostly diffuse too and the average value in the visible range is 17.25%. For the direct reflectance is 9.66%. The 11.10% left is the absorption of the material.

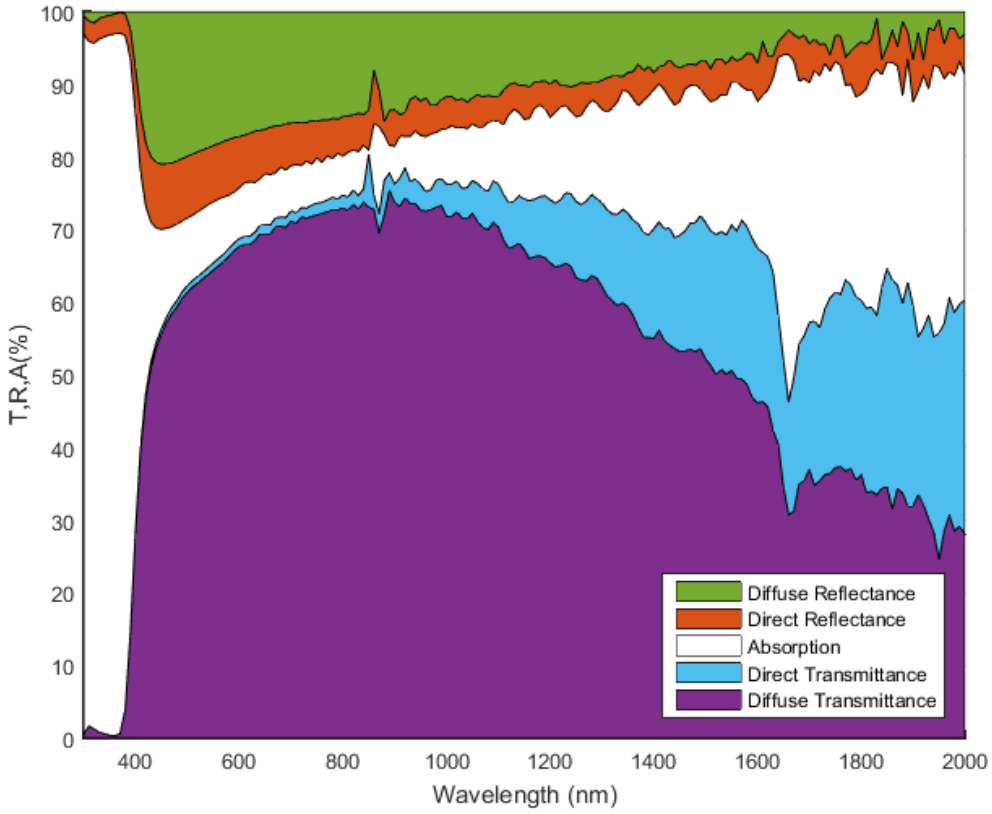


**Figure 25 Transmission, Absorption and Reflectance of self-adhesive PDLC.**

In Figure 25 the transmission, absorption and reflectance of the self-adhesive PDLC is shown. The self-adhesive PDLC refers to the one that comes with a special adhesive in the side for the user to be able to install it by sticking it into a glazing. The average values for this type of sheet are, in the visible light range: 60.26% diffuse transmittance, 16.52% diffuse reflectance, 7.12% direct reflectance and 16.10% absorption. The main difference between the types, not only in the visible range but in the whole spectrum analysed is the absorption. As it can be seen the self-adhesive type has a larger absorption mostly in the Ultraviolet (UV) range, the value here has an average of 95.41% meanwhile in the non-adhesive the average is 58.06%. This can be seen as an advantage for the users inside the buildings, because UV rays are extremely harmful for human skin, they are considered a “complete carcinogen [45].” Having a material, like the self-adhesive PDLC, that absorbs UV rays in the fenestration of buildings and houses, will reduce the need for safety measures for users and for the care of materials. The results for the complete range analysed can be seen in Table 12.

Table 12 Parameters for two different types of PDLC in OFF state

| Parameters | UV (300-380nm) | | Complete Range (300-2000 nm) | |
|---|---|---|---|---|
| | Non-Adhesive | Self-Adhesive | Non-Adhesive | Self-Adhesive |
| Direct Transmittance (%) | 0.09 | ~0 | 10.31 | 10.69 |
| Diffuse Transmittance (%) | 19.82 | 1.09 | 54.76 | 53.31 |
| Direct Reflectance (%) | 7.51 | 2.78 | 7.05 | 4.89 |
| Diffuse Reflectance (%) | 14.52 | 0.72 | 10.63 | 9.73 |
| Absorption | 58.06 | 95.41 | 17.25 | 21.38 |
| Haze (%) | 99.55 | 100 | 84.16 | 83.29 |

The haze percentage is calculated with Equation 1. The transmission haze refers to "forward scattering of light from the surface of a nearly clear specimen viewed in [terms of] transmission [46]" and it expresses the "cloudiness" of the material; how much light it scatters [46].

$$Haze\ (\%) = \frac{T_d}{T_t} \cdot 100$$

Equation 1 Haze percentage calculation

In the case of the PDLC the values are high for the opaque state, which is desirable because it acts as a barrier for the external environment: privacy is guaranteed and the transmission is mostly diffuse.

## 8.2. Mini Modules

Several mini modules were fabricated and tested in order to obtain the final design that will be used in the first prototype. In this section the evolution of the mini module design will be presented. These results regard the WACOM and the electroluminescence procedures explained in section 6.2. The first mini modules made were based on triangular solar cells, this figure was decided purely on the aesthetics of the product and the ease of manufacturing. Part of the design was to use the triangles to form other figures. The first module done with these parameters can be seen in Figure 26.

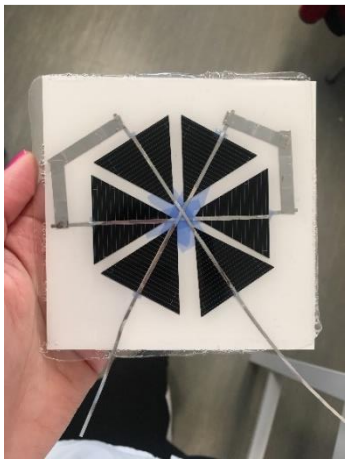

Figure 26 First mini module attempt "Hexagon Ribbon"

The electroluminescence results of this first module are shown before and after lamination in Figure 27 and Figure 28, respectively.

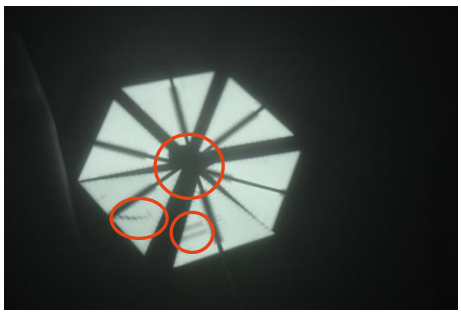

Figure 27 electroluminescence of "Hexagon Ribbon" without lamination

Figure 28 electroluminescence of "Hexagon Ribbon" after lamination

It can be seen in Figure 27 that three of the central corners of the triangles are already broken or cracked after the welding procedure. It can also be seen that in one of the cells there is a crack that starts in the busbar and in another cell there are 2 dead zones, which could be due to a crack, product of the manipulation of the device or due to manufacturing of the solar cell itself. In Figure 28, after lamination, it can be seen that no new cracks appeared which makes this design interesting for the final prototype, when is handled with care. From Figure 26 it is clear that the connections were done around the solar cells, this presents less risk of cracking due to stress concentration as a result of the copper tin-coated rod.

After some practice in manufacturing the mini modules, several other designs were made, some kept the triangular shape for the solar cells. The evolution of the design was based on how easy the manufacturing procedure was, taking into account if the solar cells broke easily or not during cutting, welding and lamination. In Figure 29, Figure 30, Figure 31 and Figure 32 different designs are shown. For these designs, electroluminescence pictures were taken and I-V curves were measured.

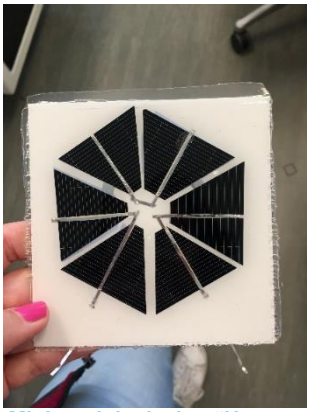

Figure 29 Mini module design “Hexagon Hidden”

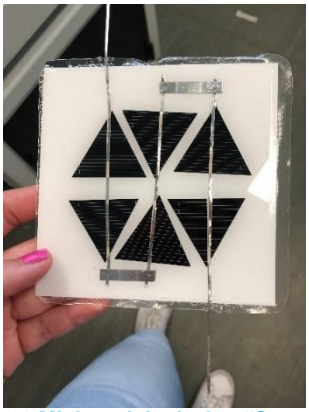

Figure 30 Mini module design “Spaceship”

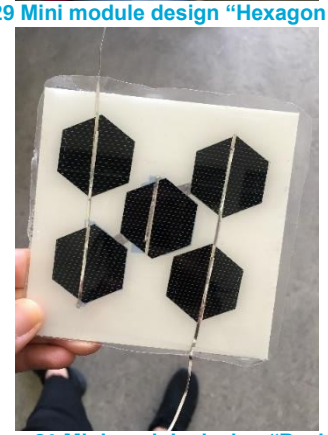

Figure 31 Mini module design “Beehive”

Figure 32 Mini module design “Hexagon Hidden 2”

The electroluminescence pictures before lamination can be seen in Figure 33, Figure 34, Figure 35 and Figure 36 and the ones after lamination are shown in Figure 37, Figure 38, Figure 39 and Figure 40.

Figure 33 “Hexagon Hidden” before lamination

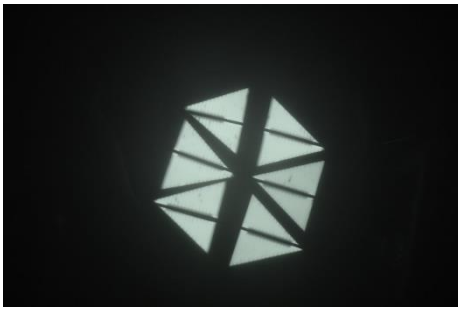

Figure 34 “Spaceship” before lamination

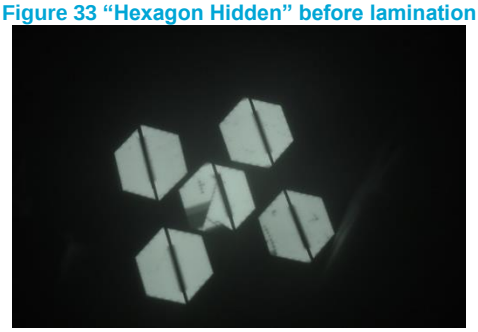

Figure 35 “Beehive” before lamination

Figure 36 “Hexagon Hidden 2” before lamination

Figure 37 “Hexagon Hidden” after lamination

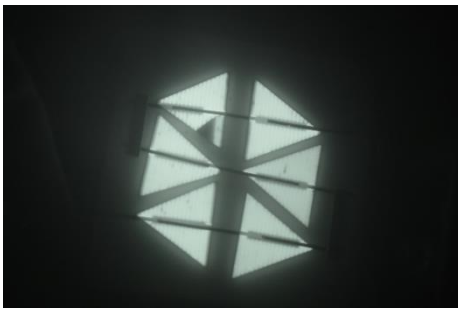

Figure 38 “Spaceship” after lamination

Figure 39 “Beehive” after lamination

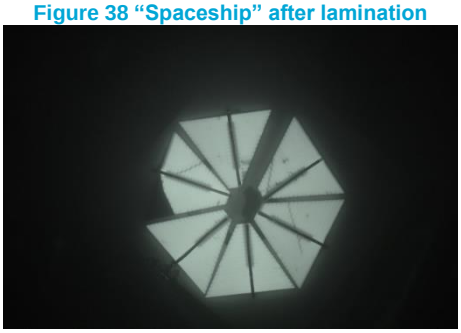

Figure 40 “Hexagon Hidden 2” after lamination

During the brainstorming of ideas, taking into account what could be aesthetically appealing from the architectural point of view, the designs shown before were made. The hexagon hidden was done in 2 different ways. The first design in Figure 29 had some visible connections in the centre of the hexagon. The second design in Figure 32 was done hiding every single connection, leaving the centre completely free. As it can be seen, the second design after lamination had more cracks than the first one, and the main reason for this to happen is because the connections in the back act as stress concentrators. The back of the mini module is uneven due to the conducting rod and increasing the amount of connections will increase the probability of the solar cells in front to break. This occurs because the lamination is done with the same pressure over the whole area. If there is a small corner that acts as a concentrating area where the force can be multiplied, there is a bigger chance that the piece that corresponds to that area breaks.

For the beehive and the spaceship designs the stress concentrators were less, due to less rod connections in the back, and in the case of the beehive the cell that was broken during welding was actually re-adjusted after lamination. This phenomenon can be seen in Figure 35 and Figure 39.

Before deciding on a design, some other considerations were taken into account, as it can be seen from Figure 26 and Figure 29 having a corner in the centre of the figure, acts as a stress concentrator. During welding is also a weak spot because many rod connections go through it. This is why trapezoids were the next shape to try, to avoid this corner loss.

The hexagons like the ones used in the beehive are more difficult to cut in the laser cuter. They need 2 more cuts compared to the trapezoid. The amount of waste that is left from cutting and hexagon from a regular square solar cell is higher. It is more difficult to optimize the area of the solar cell to obtain useful hexagon shapes. This is why trapezoids were chosen instead of hexagons.

Even though squares is the most obvious solution, aesthetically it didn’t represent an innovative design. The main concern in architecture about solar modules being used in façade is the lack of innovation in the traditionally rectangular PV modules. With this project, the exploration of other shapes and designs was possible. Such a discussion is

necessary to generate innovative designs that will attract the consumers and creators of the built environment.

Following this line of decision, the next step was to produce an amount of voltage and current enough to operate the electric circuit of the system. As it was stated before around 5 V are desired form the PV array and the current must be around 1A, all of this under STC.

The voltage values were high for these mini module designs but the current values were far from ideal. Even though at this point the electric circuit was not completely finished, values around 1A were desired because most of the electronic devices used in a PV system of this size have a minimum current input to start operating. There was a need for bigger trapezoid mini solar cells. The reason for increasing the surface area of the solar cell can be explained with the short circuit current. “The short circuit current of a solar cell depends on the photon flux incident on the solar cell [30]” so if there is more area to harvest the incident light there is more photon flow. This final design, that included bigger mini solar cells, can be seen in Figure 41. Due to restrictions in the material for lamination, mainly the corning glass, only 4 cells were used per mini module, this had an effect on the voltage that will be discussed later in this section.

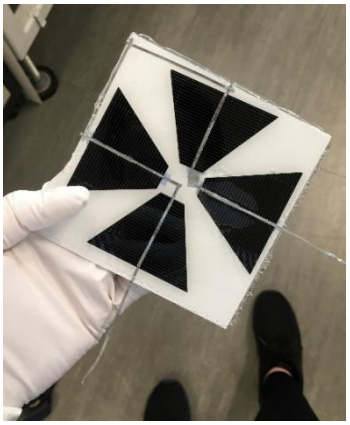

Figure 41 Final design mini module for first prototype

After selecting the final design, 8 mini modules with the same characteristics were manufactured. Not every solar cell is exactly the same, due to the artisanal manufacturing conditions. This is why the standard deviation and other size parameters of the cells were calculated and these can be seen in Table 13. In Figure 42 a sketch with the explanation of the measurements is shown.

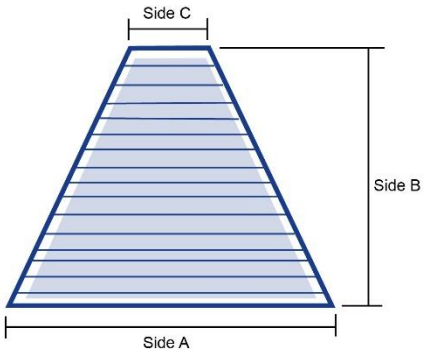


Figure 42 Sketch of a cut solar cell

Table 13 Parameters to characterize the difference in size of the cut solar cells.

| Parameters | Side A | Side B | Side C |
|---|---|---|---|
| Mean (cm) | 5.44 | 3.75 | 1.24 |
| Mode (cm) | 5.30 | 3.70 | 1.20 |
| Standard Deviation (cm) | 0.17 | 0.13 | 0.11 |
| Percentage of deviation from the mean (%) | 3.13 | 3.47 | 8.87 |

A comparison between some I-V curves of the final mini modules and the previous designs shown in this section, can be seen in Figure 43 and Figure 44. Only 4 of the 8 mini modules were compared in this graphs, the rest of the I-V curves from the complete array are shown in section 8.3.

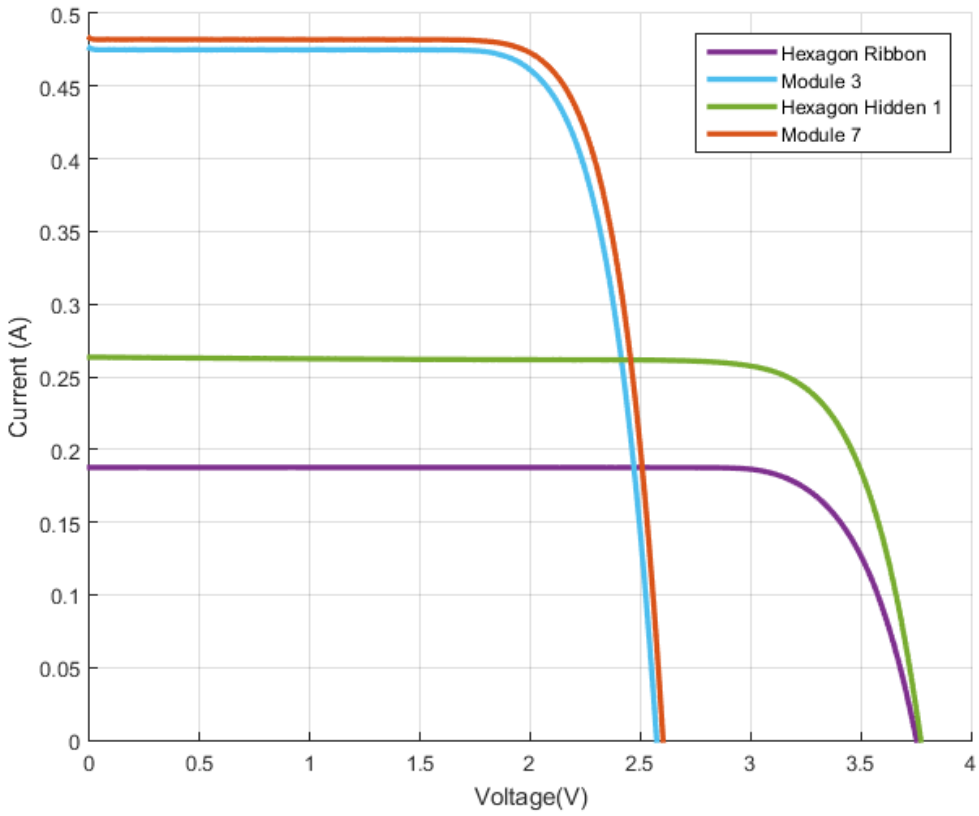


Figure 43 I-V curves of different prototypes

In Figure 43 the first design known as the “hexagon ribbon” and the “hexagon hidden 1” are compared with two of the final mini modules of the first prototype. Because of the difference in size between the final manufactured mini solar cells and some other variables that will be discussed later in this section, the curves of “module 3” and “module 7” are not exactly the same. Even though this is the case, it can be seen from the graph that both have short circuit currents close to 0.480 A. The short circuit current for module 3 is 0.476 A and 0.483 A for module 7. This increase in current compared to the previous designs has to do with the size of the solar cells and it was desirable for the final prototype. As it was explained before, in order to get enough current for the system circuit to work properly, higher currents had to be achieved under STC. It is also clear that the open circuit voltage has decreased from the first designs to the final mini module prototypes, this is due to the reduction in the number of solar cells. The main restrictive

factor was the corning glass used for lamination. The size of the glass was 10 x 10 cm and only 4 cells, from the final design, could fit these dimensions.

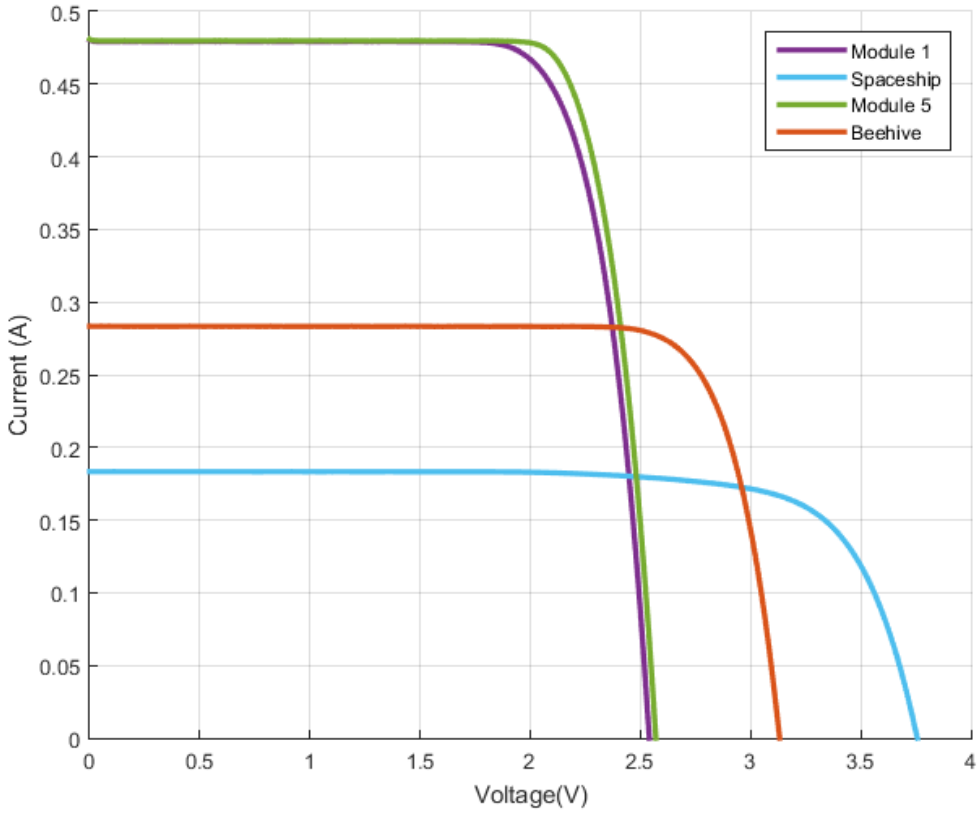


Figure 44 I-V curves of different prototypes

In Figure 44 the I-V curves for module 1, module 5 and the designs “spaceship” and “beehive” are presented. The same behaviour explained for Figure 43 is seen in this graph. The final mini module designs have higher short circuit currents and lower open circuit voltages.

The reason why the I-V curves of the mini modules are not all exactly the same will be explained briefly. Variables like the damage caused on each mini module during welding and lamination affect the overall performance of each mini module, and for each of them these cracks and handling is completely unique because they are done by artisanal manufacturing. It is important to note that in the case of this particular batch of solar cells, some of them came already with some dark spots from manufacturing. These spots could be seen during the electroluminescence procedure and are shown with more clarity in Figure 46. This also affects their performance.

Figure 45 Mini module 1 electroluminescence after lamination

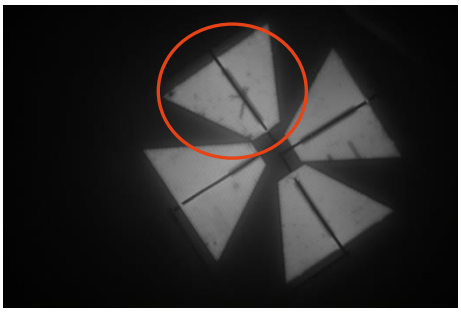

Figure 46 Mini module 3 electroluminescence after lamination

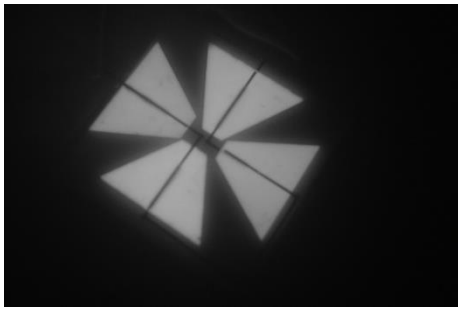

Figure 47 Mini module 5 electroluminescence after lamination

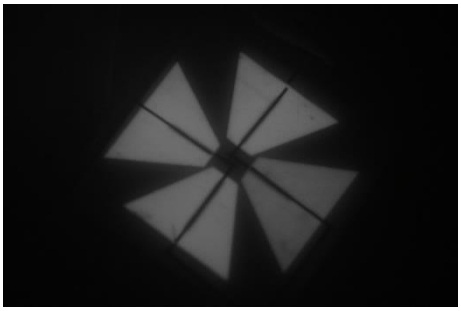

Figure 48 Mini module 7 electroluminescence after lamination

Figure 45, Figure 46, Figure 47 and Figure 48 show the electroluminescence results of 4 of the 8 mini modules used for the final prototype. The numeration of the mini modules is according to the order of manufacturing. It can be seen from these figures that in artisanal manufacturing after some practice the cracks due to mishandling of the solar cells are reduced.

## 8.3. Photovoltaic array

Two prototypes were made for this project. The mini module design for the first prototype has been discussed extensively in section 8.2. In this section the PV array made from the 8 mini modules is going to be explained and shown. Furthermore the PV array for the second prototype will be explained and the results regarding performance and aesthetics for both will be presented.

Firstly, the I-V curves of the final 8 mini modules are shown in Figure 49 and Figure 50. The modules were divided according to their current and voltage characteristics in order to maximize their performance. Because the modules are not exactly the same, the selection had to be made in a way that the ones with similar short circuit currents were together when connected in series. If this is done otherwise, the differences can be too significant and the mini module with the lowest short circuit current in a group will dictate the short circuit current of the subgroup.

The first group of mini modules are shown in Figure 49. This group is made by module 1, module 3, module 4 and module 8. The standard deviation and other parameters to show the working range of this string are shown in Table 14.

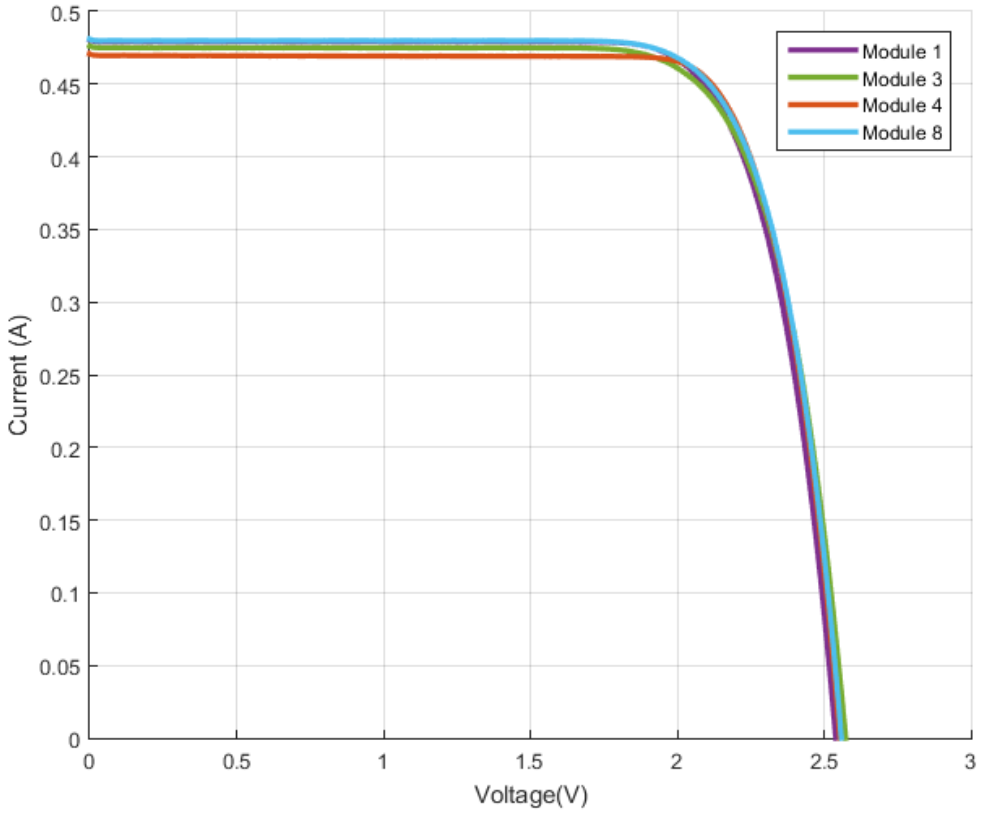


Figure 49 I-V curves under STC of group one of 4 mini modules for the first prototype

As it can be seen in Table 14, the standard deviation for the open circuit current and the maximum power point current under STC are 4.6E-3 A and 3.9E-3 A respectively. This values can be considered negligible for artisanal manufacturing because they are under 2% difference from the mean value.

Table 14 Parameters of the mini modules of group one under STC.

| | Mini Modules | | | | Mean | Standard Deviation |
|---|---|---|---|---|---|---|
| **Parameters** | 1 | 3 | 4 | 8 | | |
| Open Circuit Voltage (V) | 2.54 | 2.57 | 2.55 | 2.56 | 2.56 | 1.4.E-02 |
| Short Circuit Current (A) | 0.48 | 0.48 | 0.47 | 0.48 | 0.48 | 4.6.E-03 |
| Maximum Power Point Voltage (V) | 2.07 | 2.09 | 2.11 | 2.10 | 2.09 | 1.8.E-02 |
| Maximum Power Point Current (A) | 0.46 | 0.45 | 0.45 | 0.45 | 0.45 | 3.9.E-03 |

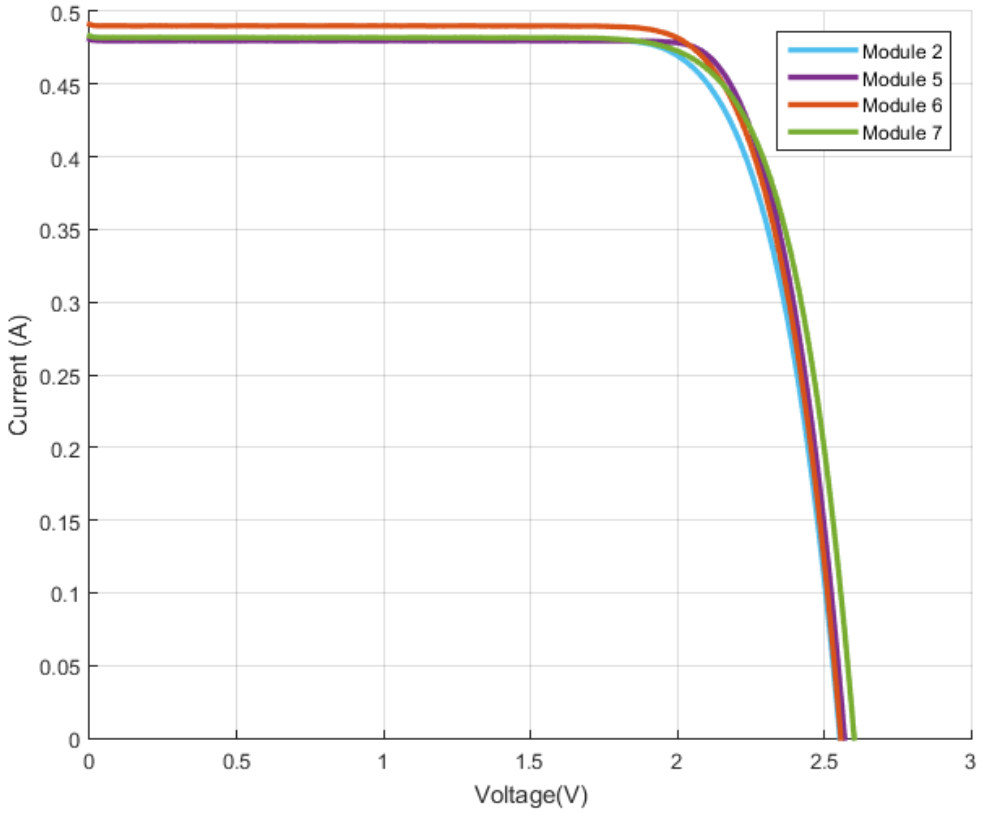


Figure 50 I-V curve under STC of group two of 4 mini modules for the first prototype

In Figure 50 the second group of mini modules is shown. This group consists of module 2, module 5, module 6 and module 7. In Table 15 some of the characteristic parameters of this batch of mini modules are shown, these were obtained under STC. The standard deviation and the mean were also calculated. In this case, the standard deviation values for current (short circuit and maximum power point) are 0.92% and 1.44% of the mean respectively.

Table 15 Parameters of the mini modules of group two under STC.

| | Mini Modules | | | | Mean | Standard Deviation |
|---|---|---|---|---|---|---|
| **Parameters** | 2 | 5 | 6 | 7 | | |
| Open Circuit Voltage (V) | 2.55 | 2.57 | 2.56 | 2.60 | 2.57 | 2.2.E-02 |
| Short Circuit Current (A) | 0.48 | 0.48 | 0.49 | 0.48 | 0.48 | 4.4.E-03 |
| Maximum Power Point Voltage (V) | 2.08 | 2.12 | 2.09 | 2.13 | 2.11 | 2.5.E-02 |
| Maximum Power Point Current (A) | 0.46 | 0.47 | 0.47 | 0.45 | 0.46 | 6.6.E-03 |

In Figure 51 the final ***PV array for the first prototype*** is shown. The interconnection between the mini modules is the following: each group of modules are connected in series and the two groups obtained are connected in parallel between them. This means that the lowest current of the series group will be the circuit current of the string and then, when connected in parallel, this current values will be added. For voltage, each module

will add to the voltage of the series string and when connected in parallel the minimum voltage between the two strings will be the final voltage of the array. The schematics of the connection that was just explained are shown in Figure 52.

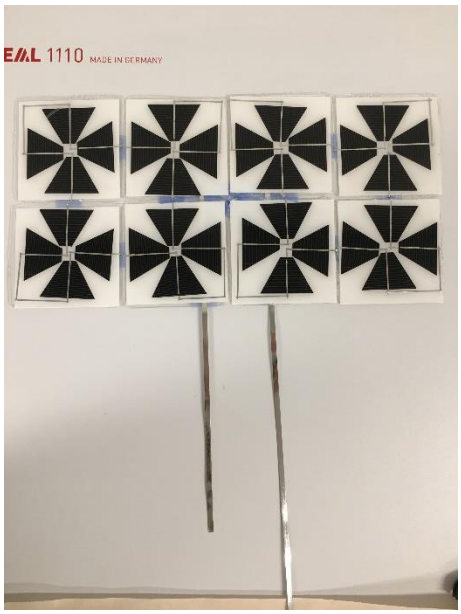


Figure 51 PV array for the first prototype

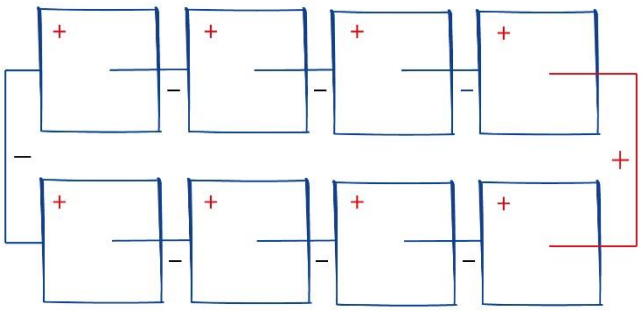

Figure 52 Sketch of the connection between the mini modules of the first prototype

The array shown in Figure 51 was characterized in the Large Area Steady State Solar Simulator (LASS). This device, as the name states, simulates the solar spectrum with the help of halogen lamps, gas lamps and mirrors. The class of this simulator is *AAA*, like the one used for the characterization of the mini modules explained in section 6.2. This class is the best classification for a solar simulator and these devices are used mostly for research. The software used with the ***LASS*** is ***ReRa Tracer 3***. In the software some parameters of the module that will be characterized have to be entered. In the case of the mini module array for the first prototype the information entered can be seen in Table 16.

Table 16 parameters of the PV array for the first prototype

| | Values |
|---|---|
| Module area ($m^2$) | 0.08 |
| Cell area ($cm^2$) | 12.54 |
| Strings per module (-) | 2 |
| Cells per string (-) | 16 |

The result of this characterization, is the I-V curve of the array and it is shown in Figure 53. The power delivered vs. voltage (P-V) curve is shown in Figure 54. The irradiance was close to STC and it was 997.75$\frac{W}{m^2}$, it had an error of 0.23%.

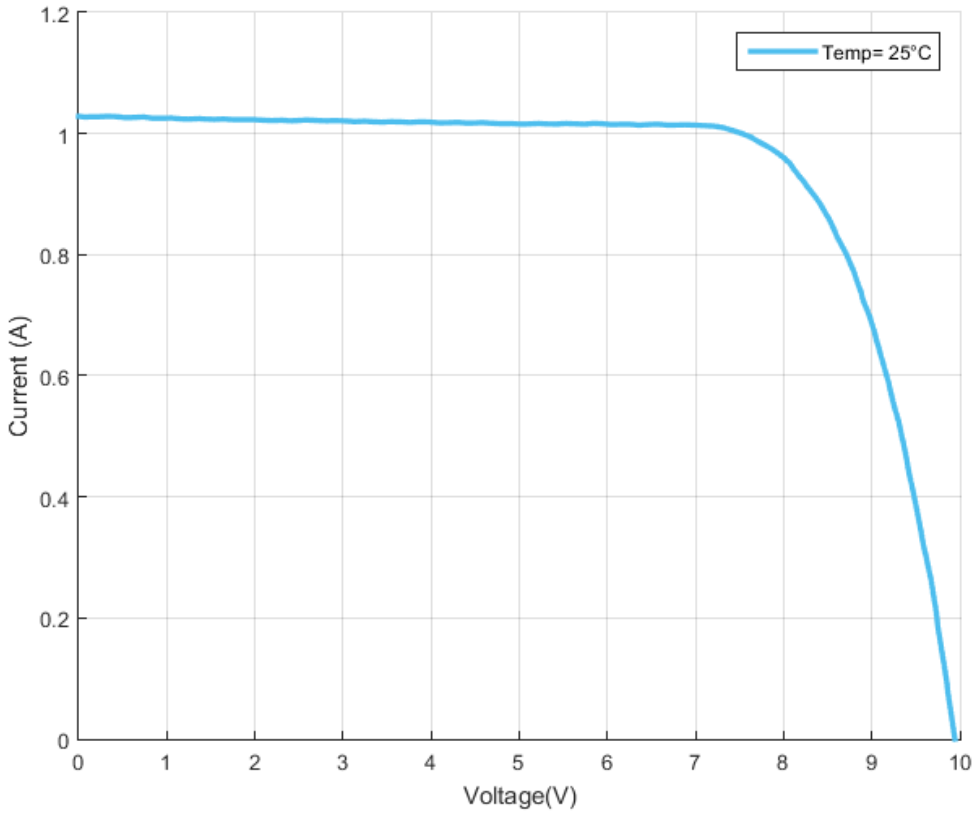


Figure 53 I-V curve under STC of the PV array for the first prototype

From the curve obtained, shown in Figure 53, some important characteristics of the array can be determined. The open circuit voltage of the array is 9.94 V, the short circuit current is 1.03 A which is around the value expected to have a secure supply of current for the electric circuit of the system. All the characteristics of the PV array are presented in Table 17.

Table 17 Characteristics of the PV array for the first prototype

| | Values |
|---|---|
| Open circuit voltage (V) | 9.94 |
| Short circuit current (A) | 1.03 |
| Maximum power point voltage (V) | 7.95 |
| Maximum power point current (A) | 0.97 |
| Fill Factor (%) | 75.00 |
| Efficiency (%) | 19.11 |

Based on Table 14 and Table 15, it is possible to compare the expected behaviour of the array, only with the information of the modules, and the characterization in the LASS of the connected array shown in Table 17. The expected open circuit voltage of the array, taking into account the information of each individual module and the intended connection explained in Figure 52, is 10.23 V. This voltage differs in 2.84% from the one calculated with the LASS. The short circuit current is 0.95 A and the difference from the

final value is 7.77%. The maximum power point voltage and current are 8.38 V and 0.90 A. This values differ in 5.41% and 7.23% from the values measured in the LASS, respectively.

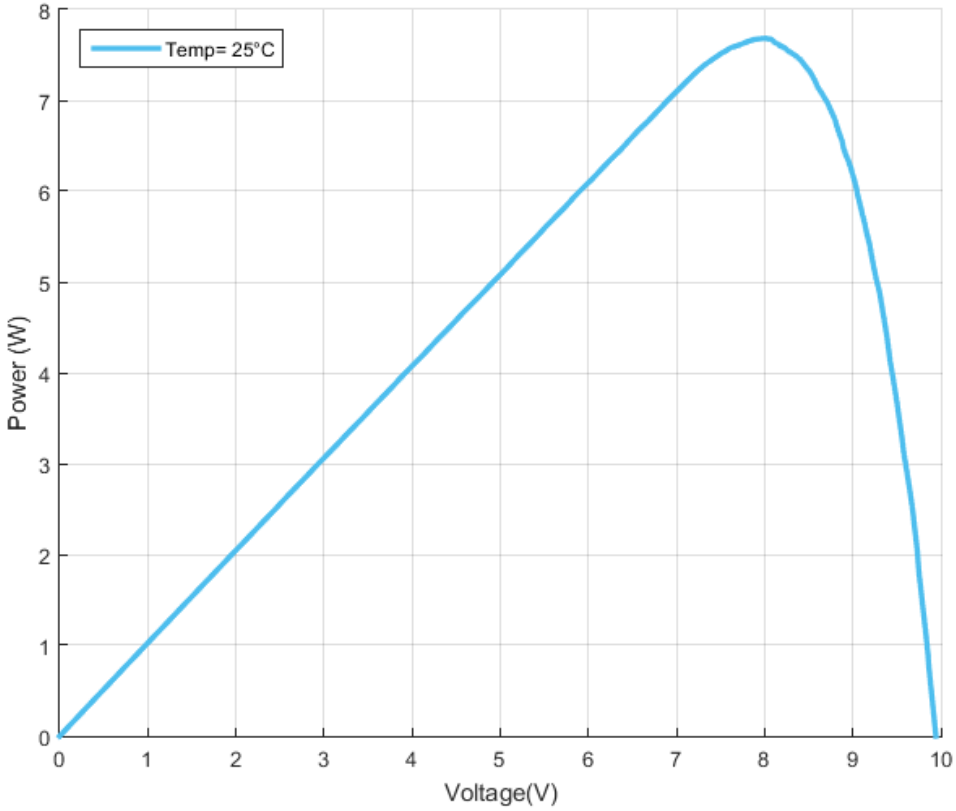


Figure 54 P-V curve under STC of the PV array for the first prototype

In Figure 54, the P-V curve of the array is shown. The P-V curve is used to know the power delivered by the array or the module under STC conditions. When the PV device is connected to a load the operating voltage is dictated by the load and this is why the curve is used to know the operating point of the array under certain load condition [30]. To operate at maximum power point the array has to be forced to work at maximum power point voltage, the way to do this is with an MPP that was explained in section 5.2. The maximum power point delivers 7.67 W and it corresponds to the maximum power point voltage showed in Table 17.

The ***second prototype PV array*** is now going to be discussed. In the case of this prototype, previous mini modules were not made. This is why it is only explained in this section. The array for this model can be seen in Figure 55.

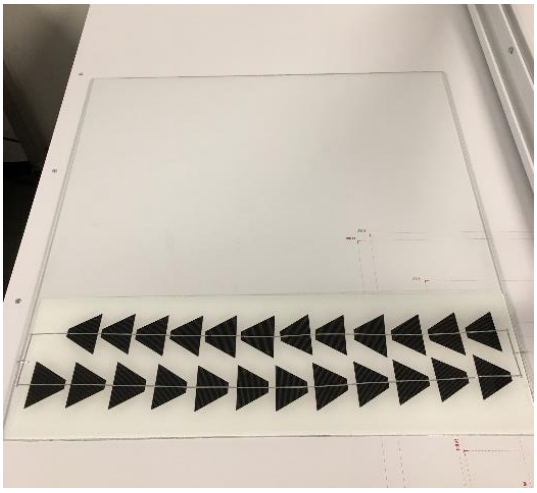

Figure 55 Second prototype PV array

The PV array shown in Figure 55 is constructed with the same solar cells used for the first prototype. In this case 1 string of 12 cells was connected in parallel to another string of 12 cells. The parameters entered in the software of the LASS for the second prototype are shown in Table 18.

Table 18 parameters of the PV array for the second prototype

| | Values |
|---|---|
| Module area ($m^2$) | 0.12 |
| Cell area ($cm^2$) | 12.54 |
| Strings per module (-) | 2 |
| Cells per string (-) | 12 |

This array was also characterized and the results of the I-V curve can be seen in Figure 56. For this particular case, the LASS had one light bulb off, so the irradiance was 888.76$\frac{w}{m^2}$. The software used, corrects the curve for irradiance and temperature and it calculates how the curve will look under STC. The temperature was 25.79 °C and it was also corrected.

Table 19 Characteristics of the PV array for the second prototype

| | Values |
|---|---|
| Open circuit voltage (V) | 7.73 |
| Short circuit current (A) | 1.14 |
| Maximum power point voltage (V) | 6.16 |
| Maximum power point current (A) | 1.09 |
| Fill Factor (%) | 76.46 |
| Efficiency (%) | 22.33 |

The same analysis done for the first prototype was done for the second prototype. In Figure 56, the I-V curve is shown and as it can be seen, it has a lower open circuit voltage than the first prototype. The open circuit voltage for the second array is 7.73 V. The short circuit current in the other hand is higher for this prototype with a value of 1.14 A. The complete list of characteristics of the PV array is shown in **¡Error! No se encuentra el origen de la referencia.**.

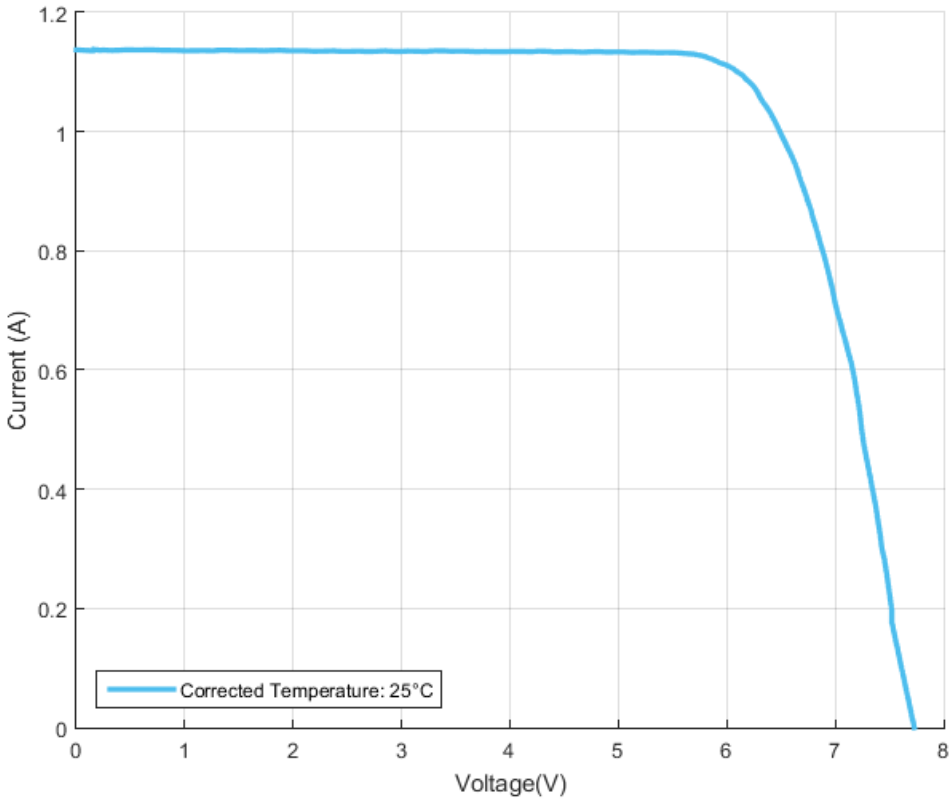


Figure 56 curve under STC of the PV array for the second prototype

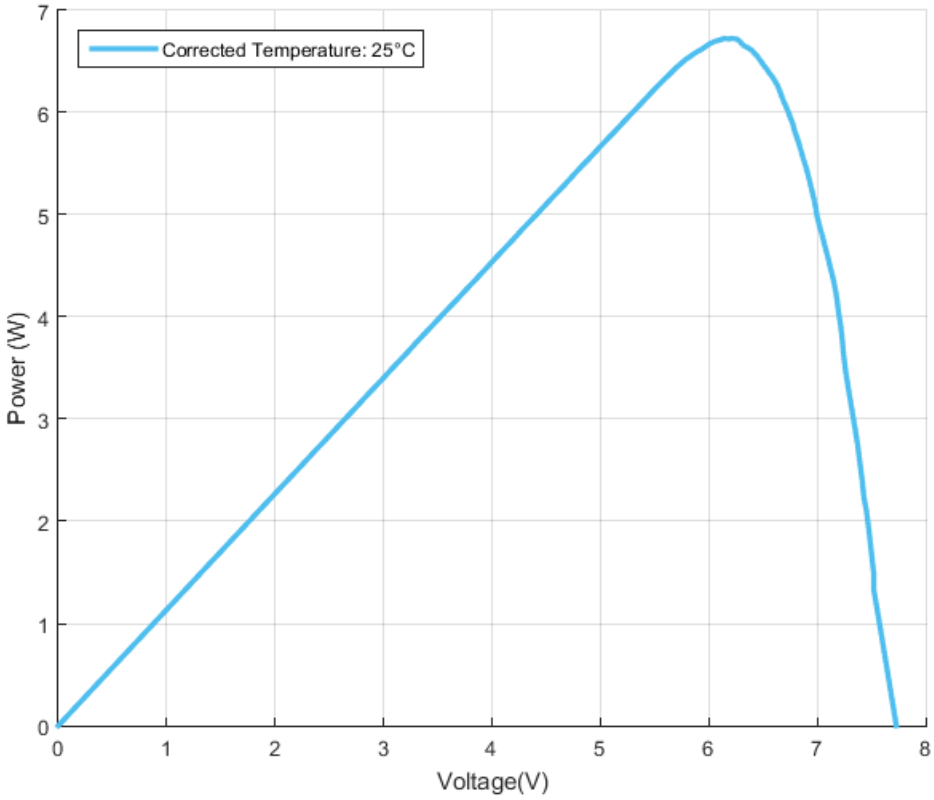


Figure 57 P-V curve under STC of the PV array for the second prototype

In Figure 57, the P-V curve for the second prototype is shown. The maximum power point of this array is 6.72 W, around one watt lower than the first prototype. Even though the voltage and power characteristics of this prototype are lower than in the case of the first prototype, the fill factor and the efficiency are higher. There is a better use of the area and the quality of the materials and manufacturing is probably better.

# 9 Manufacturing

In this chapter, the manufacturing process of the mini modules, testing bench and smart windows will be explained. These procedures were done in the facilities of the PVMD department.

## 9.1. Mini Modules

To create the mini modules, 3 main steps had to be followed: the laser cutting of the original square solar cells, the welding of the busbars to the new cells along with the welding of the module circuit, and finally the lamination of the mini module.

First, the Al-BSF solar cells were located in the ***cutting chamber***. The cutting chamber consists of a polymer rectangular prism with green semi-transparent walls. Inside, there is a mechanically-adjustable platform with a point grid. This chamber and the set up for laser cutting can be seen in Figure 58. Inside the chamber, a camera is located pointing directly to the platform, giving a top view of the sample. After locating and adjusting the platform to the view in the software, the pattern desired is designed virtually.

**Figure 58 Laser cutting set up**

Before reaching the final design, some of the concept designs were tested. In this case figures like trapezoids, triangles and hexagons were patterned in the square Al-BSF cell. After creating the design, trying to keep the material waste as low as possible, the laser cut is done. The parameters for the laser cutting are adjusted according to the tests realized by Arturo Martinez in his thesis project. The parameters can be seen in Table 20.

**Table 20 Parameters for the laser cutting of AL-BSF solar cells**

| Parameter | Value |
|---|---|
| Repetitions (-) | 100 |
| Frequency (Hz) | 325 |
| Ton (ns) | 20 |
| Power (%) | 100 |
| Speed (mm/s) | 2000 |

The second step is to weld the busbars to each individual cell, as well as making the mini module connections. The ***welding*** is one of the key points of the artisanal manufacturing procedure of the mini modules. This step is where the solar cells can be cracked the most because of human error.

To weld the copper tin-coated rod to the solar cell, it is necessary to clean every surface that will be in contact with the soldering. These surfaces are: the solar cell original busbar and the welding tip. The solar cell surfaces are cleaned with *No clean flux dispensing pen* manufactured by Chemtronics. The cleaning has to be done for every cell on both sides, negative and positive. In Figure 59 the welding procedure is shown.

**Figure 59 Solar cell and mini module welding procedure**

The final step in manufacturing is ***lamination***. For lamination several materials are needed. These materials are:

- Corning Glass
- Ethylene Vinyl Acetate
- Tedlar (white or black colour)

The ***corning glass*** is the layer that protects the mini module's front part. The front is the harvesting area of the solar cells. Solar cells must be encapsulated, because they are brittle devices and if their metallic contacts are exposed to humidity, they will deteriorate fast. This is why it is necessary to protect them with a material that allows the solar spectrum to cross through it, minimizing parasitic absorption as much as possible.

Ethylene vinyl acetate copolymer most commonly known as ***EVA*** is the material that encapsulates the mini module. It is used at the front and the back of the PV module and it has some unique properties that will be explained briefly. It is first, a "self-priming [material] for adhesion to glass [47]" this means that doesn't need any other materials to adhere to that surface. The one used for this project is the Photocap 15580 P from STR holdings. It has a tensile strength of 15 MPa and an optical transmission of 91%. The refractive index of this material is 1.48 [47]. All these optical properties are relevant for the module design because they are related to the transparency of the material, necessary for the solar cells to harvest as much photons as possible. The tensile strength is more related to the durability of the mini module which for the case of the prototype is not very relevant but for a real product is imperative.

Finally ***Tedlar*** is used for the back of the solar cell. Tedlar is also known as polyvinyl fluoride or PVF and it has specific properties that protect the PV module in different ways. It is used to isolate the rear of the module from moisture that can be found in the mounting. It also protects it from UV and thermal degradation. For this project the white

colour was used. The selection was made because of aesthetical reasons but an advantage of the white Tedlar is that it reflects some of the light that wasn't harvested by the solar cells in the first pass. This property increases the chances of the light to be harvested by the mini module in a second pass.

For creating the module using all these materials, a laminator is needed. The PVMD group has an ***Experia Photovoltaic Laminator.*** The area of lamination is 60 x 60 $cm^2$, this is why the prototypes have these dimensions. In Figure 60 the laminator is shown.


**Figure 60 Experia Photovoltaic Laminator**

The laminator has several stages and for each stage parameters like pressure and temperature are defined. The lamination of the mini modules has to be done under certain conditions, because the materials explained before have specific melting points and can only handle certain pressures without breaking or cracking. The stages and the different parameters of lamination are shown in Table 21.

**Table 21 Standard Recipe for lamination of mini modules with AL-BSF**

| Step | Time (s) | Pressure Up (mbar) | Pressure Down (mbar) | Temperature (°C) | Remarks |
|---|---|---|---|---|---|
| 1 | - | 1000 | 1000 | 140 | - |
| 2 | 120 | 0 | 0 | 140 | Evacuating |
| 3 | 500 | 0 | 0 | 140 | Heating up |
| 4 | 60 | 150 | 0 | 140 | Compressing |
| 5 | 500 | 150 | 0 | 145 | Curling |
| 6 | 30 | 0 | 1000 | 145 | Venting |
| 7 | 30 | 0 | 1000 | 145 | Release |
| 8 | 9999 | 1000 | 1000 | 60 | End of recipe |

To begin with the lamination process, it is necessary to clean every layer and organize them. The first layer is the glass. It is placed facing down in the laminator. The next layer is the EVA and then the PV mini module. After the PV mini module another EVA layer is placed and to close the bundle the Tedlar is used.

## 9.2. Testing Bench

For future assessing of the viability of the prototypes in the built environment a testing bench was made. The testing bench was based on the PASSYS test cells that were

developed in Europe in 1994. The PASSYS test cells “are outdoor facilities for the evaluation of the thermophysical parameters of real scale samples of façades and building components [48].” But the most important application of these testing cells is for assessing “passive solar façades [48]” like in the case of this project.

The PASSYS test cells were developed for testing big scale prototypes and were located all across Europe. In the Netherlands the organization TNO used to have one, unfortunately they don’t have it anymore. The volume of these cells was 38 $m^3$ and the floor area was 13.8 $m^2$. The walls, floor and ceiling were made of a layer of mineral wool (80 mm width) and polystyrene foam (30 cm width). The room was sealed so the air change rate was less than 0.01 $\frac{L}{h}$. The walls inside were painted with 0.8 reflectance value matt white paint [48].

Based on this information a testing bench was constructed. First of all, this testing bench was made for prototypes of 60 x 60 cm, this means that it can have a smaller volume. A smaller testing bench is advantageous for the PVMD group because of the space shortage there is. This is why the testing bench has a volume of 0.38 $m^3$. The sketch of the prototype with the dimensions can be seen in Figure 61.

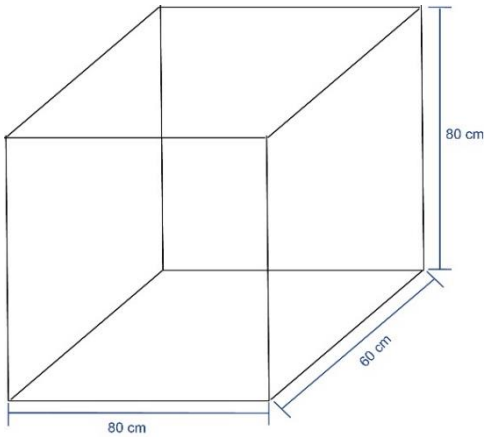


Figure 61 Sketch dimensions testing bench

The materials used for this testing bench are as follows. For the walls, the floor and the ceiling 22 mm width Medium Density Fibreboard (MDF) is used. All the corners and vertices of the bench are closed with isolating tape. The testing bench has wheels at the bottom, for easy transport, and the front wall has a slit to fit the prototype and be able to change it in the case that other ideas or designs want to be tested in the future. The front wall dimensions are shown in Figure 62.

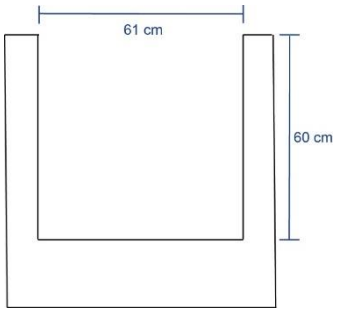


Figure 62 Front slit for the smart window prototype to adjust in the testing bench

The walls were joint together with special MDF extra strong glue and screws. After this, metal angles were placed in the vertices to give extra support. The testing bench construction process is shown in Figure 63 and Figure 64. For the internal walls, white

paint was used. The specifications of the paint are shown in Table 22.The final result of the testing cell is shown in Figure 65.

**Table 22 Information about the paint used for the testing bench**

| | Values |
|---|---|
| Reference | RAL 9010 - RAL Classic Pure White |
| Light Reflectance Value | ~0.84 |
| sRGB | 240; 237; 225 |

**Figure 63 Construction of the testing bench**

**Figure 64 Construction of the testing bench**

**Figure 65 Testing bench final result**

## 9.3. Smart Window

For this project two prototypes were made. The first prototype array was adhered to the glass by mechanical means. The second array was laminated into the final glass directly. The procedure for both prototypes will be explained below.

The first prototype array was glued into the glass with Loctite Super Bonder glue. This is a special glue used in several industries because of its fast and unique formula that adheres very well. In the case of the second prototype the lamination procedure explained in section 9.1 was done with the full 60 x 60 glass.

The PDLC used for both prototypes was the self-adhesive. This was the final decision due to the incompatibility of the EVA with the non-adhesive PDLC. The non-adhesive

PDLC has to be laminated at maximum 130°C and the EVA available in the PVMD group has a nominal temperature for lamination between 145-150° C. The EVA is also needed between the PDLC and the glass as a self-priming material. These are the reasons why only self-adhesive PDLC was used. The final prototypes, one and two, are shown in Figure 66 and Figure 67, respectively.

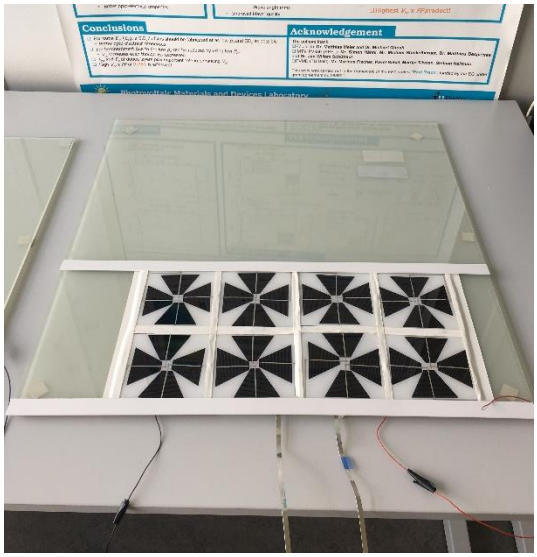


Figure 66 Final prototype 1

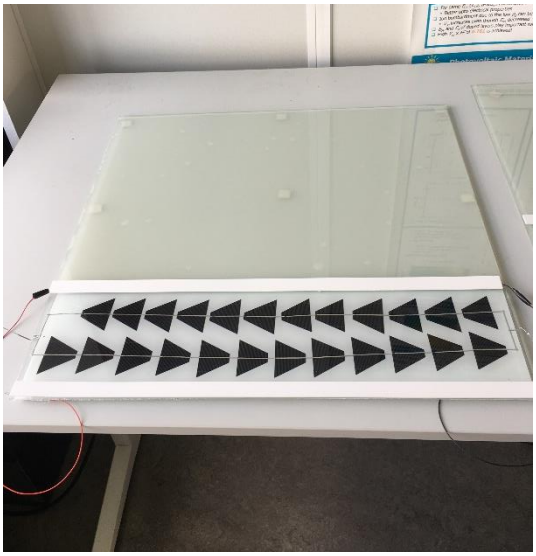

Figure 67 Final prototype 2

# 10 Smart window testing

The final stage of the project was to assess the feasibility of the PV system. To achieve this, the smart window and the balance of system had to be connected and tested outside the PV laboratory of the PVMD group. To assess the system in a real case scenario with different shading conditions, several simulations in System Advisor Model (SAM), a software from the National Renewable Energy Laboratory (NREL), were done. In this chapter both procedures will be explained in detail.

## 10.1. Prototype testing

After acquiring all the subsystems, some of them had to be adjusted to fit the energy requirements and physical constraints of the design. Subsequently, they had to be connected together to build the off-grid PV + PDLC system.

In section 6.3, the schematics of the off-grid PV system circuit were shown. In this section the final system can be seen in Figure 68. For this test, closed lead gel solar batteries were used. These batteries were available in the PV lab and the manufacturing company is IKS Photovoltaik. Each battery has a nominal voltage of 12 V. Even though these batteries were used for the test, the final batteries for the PV system are the Duracell solar which were explained in section 6.3. The main electronic devices are shown in Figure 69 and Figure 70.

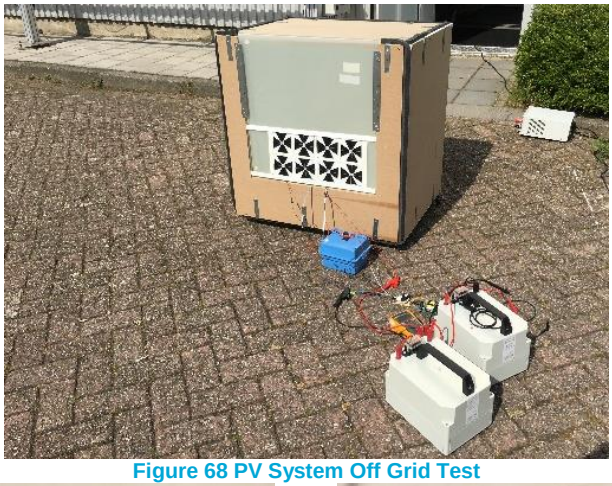

Figure 68 PV System Off Grid Test

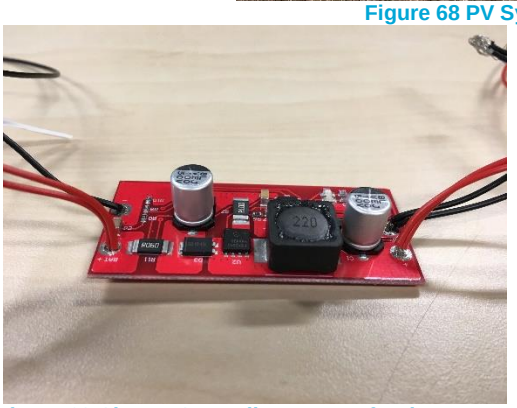

Figure 69 Charge Controller – MPPT for the system

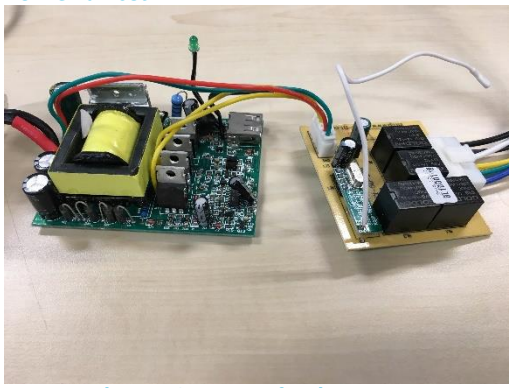

Figure 70 Inverter for the system

To show that the system can be operated in Delft, it was tested under the environmental conditions shown in Table 23, the 18th of June 2019 at 17:02. These values were

obtained from the PVMD monitoring station [49]. In Figure 71 and Figure 72, respectively, the working states OFF and ON of the window are shown.

Table 23 Weather conditions for the test of the PV + PDLC system in Delft [49]

| Parameters at 17:02 in Delft | Values |
|---|---|
| Direct Irradiance (W/m$^2$) | 183 |
| Diffuse Irradiance (W/m$^2$) | 387 |
| Total Irradiance (W/m$^2$) | 570 |
| Free Air Temperature (°C) | 29 |
| Wind Speed (m/s) | 0.9 |
| Humidity (% RH) | 42 |

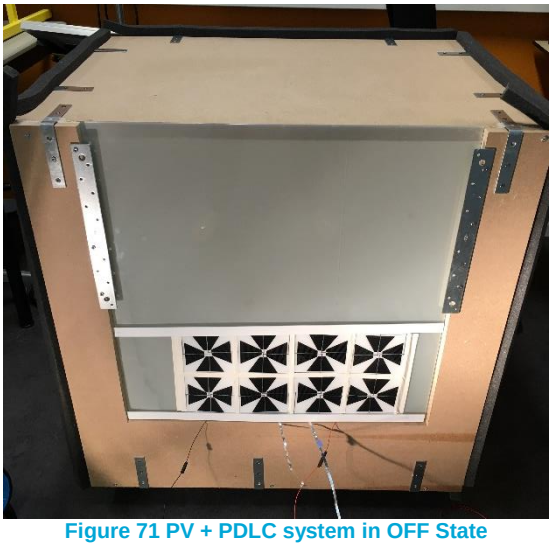

Figure 71 PV + PDLC system in OFF State

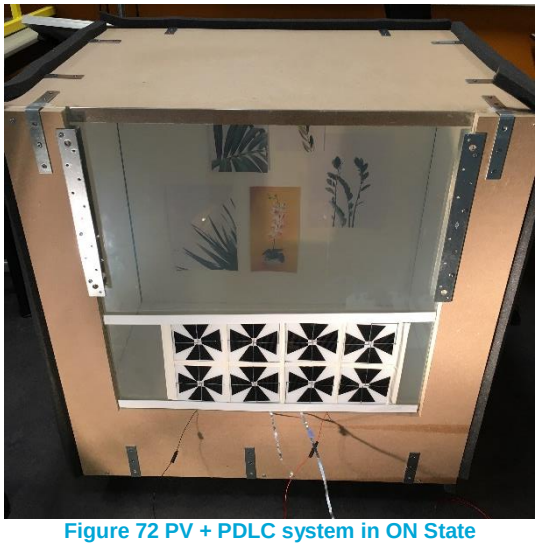

Figure 72 PV + PDLC system in ON State

During this test the instant short circuit current and open circuit voltage produced by the PV array where measured and the values can be seen in Table 24.

Table 24 Values of current and voltage measured during the prototype testing.

| | Values |
|---|---|
| Instant Short Circuit Current (mA) | 86.05 |
| Instant Open Circuit Voltage (V) | 9.57 |

## 10.2. Simulation Overview

To assess the feasibility of the PV + PDLC system, several simulations were run for a range of shading conditions. The simulations where made using as a model, a real life house, its location and surroundings. The software used is Simulation Advisory Model (SAM). This software was developed by NREL and it is a “techno-economic model [50]” that is used to “facilitate decision making for people involved in the renewable energy industry [50].” The advantage of the software is that it comes with a user-friendly interface and it has different features needed for this type of project. For the shading sensitivity analysis, it provides a 3D modelling tool where several objects can be modelled simply, like trees and neighbouring houses.

The building chosen for the project is a house-shop in Delft, Netherlands. The address is *Achterom 94* and the front view and some neighbouring houses are shown in Figure 73. The house is the second one from left to right in this figure.

Figure 73 Location for the 3D real life model assessment of the PV + PDLC system

As it can be seen, the house selected has 3 floors and in the ground floor 5 small windows can be identified. One of these windows will be modelled as the smart window from this project and the energy exchange will be assessed for a whole year in SAM.

The conditions for the model and the input variables will be explained in detail in this section. First, the location is Delft, Netherlands. The average relevant environmental characteristics of this place for a whole year are shown in Table 25. The data needed for the analysis was downloaded from *Meteonorm* [51].

Table 25 Daily average ambient characteristics for a year in Delft, Netherlands.

| Average Daily for a Year | Values |
|---|---|
| Wind Speed (m/s) | 4.47 |
| Ambient Temperature (°C) | 10.46 |
| Global Horizontal Irradiance (W/m$^2$) | 121.68 |
| Diffuse Horizontal Irradiance (W/m$^2$) | 63.84 |
| Direct Normal Irradiance (W/m$^2$) | 114.21 |

Secondly, the azimuth of the module is determined by the normal vector of the front windows in the house, with respect to the north. In Figure 74, the normal vector angle of the window with respect to the north is sketched, the image is taken from Google Maps [52]. For this project, north is taken as 0°, east is 90°, and south is 180°. The angle of the module is determined by the angle of the windows that in the case of the selected house is 90°. In Table 26, the summary of the azimuth and the module angle is shown.

Table 26 Summary of position of the module in the selected location.

| | Values |
|---|---|
| Module Azimuth (°) | 58.74 |
| Module Angle (°) | 90.00 |

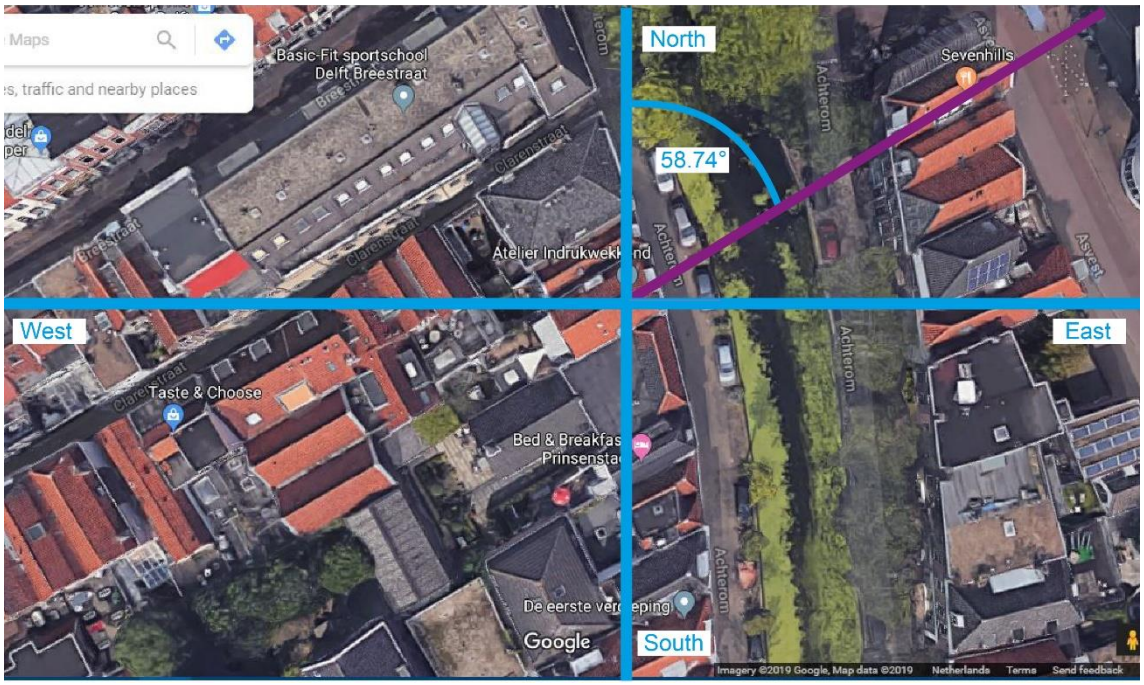


Figure 74 Azimuth of the PV + PDLC smart window in the selected location. Adapted from [52].

SAM allows the user to create a simple 3D model to determine the shading conditions of the panel. In Figure 75, the model done for this project is shown. The red spot at the left indicates the location of the module. This spot can be seen in front of the orange roof (indicated with a red arrow), which represent the house where the smart window is going to be assessed.

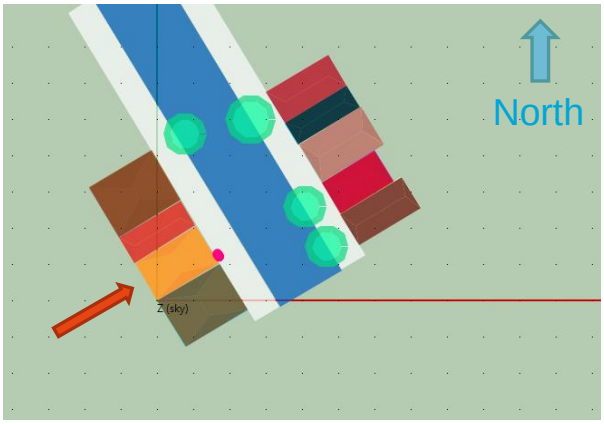


Figure 75 Top view of the 3D model for real shading conditions of the prototype

The 3D model shown in Figure 75 was based in the field pictures that are shown in Figure 73, Figure 76, and Figure 77, among others. The length and width of the houses was calculated with Google Maps “measure distance” tool and the height was approximated with the average height of 1 floor in the Netherlands which is around 3 m [53]. For the trees the height was calculated using the field pictures by comparing the trees with the houses close by. This location was also chosen because the azimuth is far from optimal for Delft, which will serve as a radical case for the assessment of the smart window. To assess the feasibility of the PV + PDLC system, a common scenario in an accessible location was chosen.

Figure 76 Field research photograph for the creation of a 3D model in SAM

Figure 77 Field research photograph for the creation of a 3D model in SAM

After selecting the location and assessing the shading conditions, the load is modelled for each hour of a year. To obtain a model that is as close to reality as possible the load conditions, to which the PV system is going to be subjected, have to be input. The only load this PV system has is the PDLC when it is switched on. The power the film of 60 x 60 cm consumes is 1.332 W. To do a load model, it was decided that weekdays and weekends were going to be simulated under different triggering conditions and a typical day of each of this cases for every month was going to be created. After the typical days for each month were modelled, they were repeated for a whole year to obtain 8760 data points. The construction and control decision for the PDLC switching load model will be explained below.

During weekdays, the plane of array (POA) beam irradiance after soiling and shading is used. This irradiance is “incident on the plane of the photovoltaic array in a given time step [54].” The word beam refers to the direct component of the irradiance. The array and the window are located in the same position, this means that a direct beam of irradiance will activate the PDLC and make it transparent. This control decision was based in maximizing the use of natural light, an important variable for the location selected. This decision will likely reduce the need of heating in winter but will likely increase the use of air conditioning in summer. However, for the scope of the project, heat transfer is not a variable taken into account. Later in this document, it is suggested that a more complex control system for the PDLC is implemented.

During weekends, the triggering environmental condition is ambient temperature. This decision is aimed to ensure comfort in the coldest months yet still reduce the need for artificial lighting. When the ambient temperature is over 20.25 °C, the PDLC will become transparent. This value of temperature is the mean of the average highest temperature in May, June, July and August in Delft. These values are obtained from the National Oceanic and Atmospheric Administration (NOAA).

These months were selected because there is a single control decision for the whole year for this particular system. This means that every month will work with this reference value. If a lower value is selected, for example, the average of the winter months, the PDLC will be transparent for every hour of every day during the summer months. In this situation, in the weekends, when less people are working inside the shop, there will be more energy wasted because there is no need for transparent windows. In Figure 81 the modelled week for January and July are shown.

The shading sensitivity was tested with 3 scenarios other than the one shown in Figure 75. This 3 scenarios where based on the model explained above. Each scenario was done using the same location and surroundings but a few shading elements were deleted until one without buildings and trees was modelled. The 3 sensitivity scenarios are shown in Figure 78, Figure 79 and Figure 80.

For each scenario, including the full model, results of the interaction with a “grid” and shading factors will be explained in section 10.3.

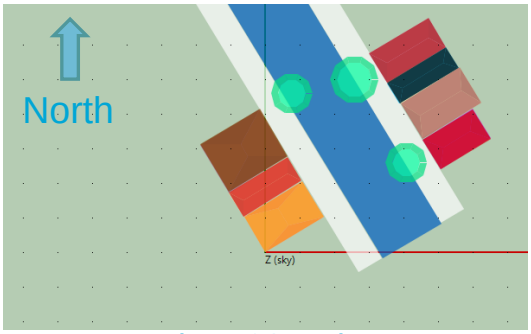


Figure 78 Scenario A

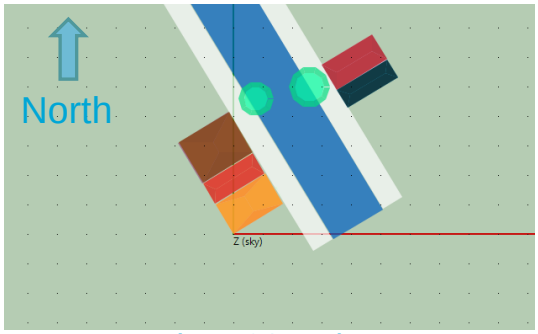


Figure 79 Scenario B

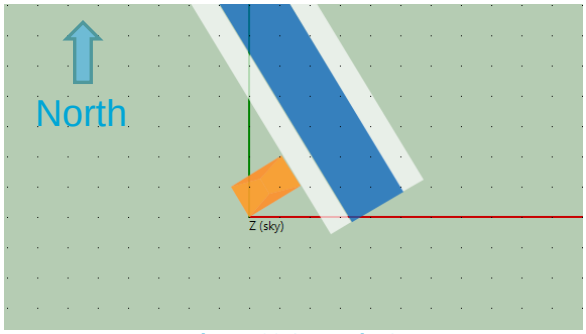


Figure 80 Scenario C

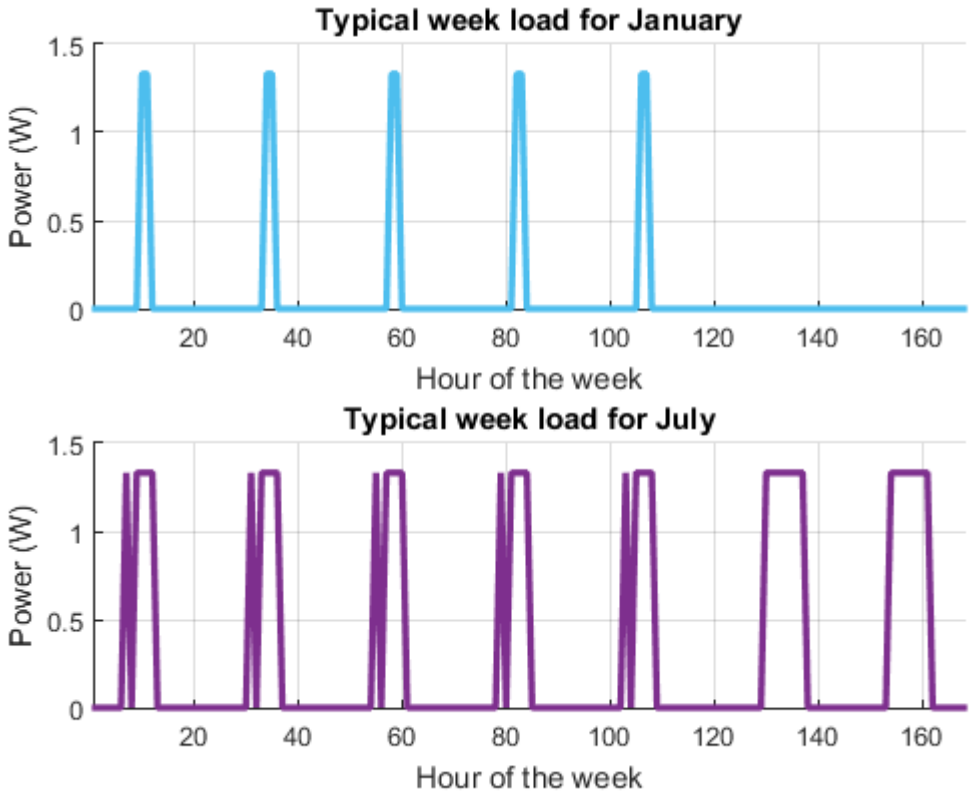


Figure 81 Week load model for January and July

## 10.3. Simulation Results

The simulation results give a very positive light to the project. The feasibility of a market product that involves the integration of PV arrays into building façade is high. The reasoning will be explained along this section.

The real scenario, where all the shading elements are considered needs energy from the grid 38 hours of the year. This means 0.43% of the amount of hours in a year. This is shown in Table 27. Because this is an isolated window in a specific case this values could vary greatly, but several things can be pointed out for this case that can improve the values obtained from the simulation, as it will be explained bellow.

First of all, in the case of this particular shop, the other 4 windows can also be used as smart windows. Each window is subjected to different shading conditions and between them there is a possibility that they can harvest enough energy to work together and not rely on the grid. Secondly, other windows in higher floors in the building can be considered. Choosing windows in higher locations can result in less shading, meaning better harvesting of sunlight and functioning of the PV array.

In Figure 82, the state of charge of the bank of batteries for the full model scenario is shown. As it can be seen, the charge of the battery is limited by the minimum and maximum state of charge that in this case were chosen to be 15% and 95%, respectively. If this figure is compared to Figure 83, it can be seen that in the first few hours the grid has to enter into the system and the battery is depleted. This is an expected behaviour, because even though the model was started with fully charged batteries (95%) it is started the 1st of January, when the irradiance in the Netherlands has the lowest values. If the model is started in July the behaviour will be completely different because the irradiance around this month reaches the highest values.

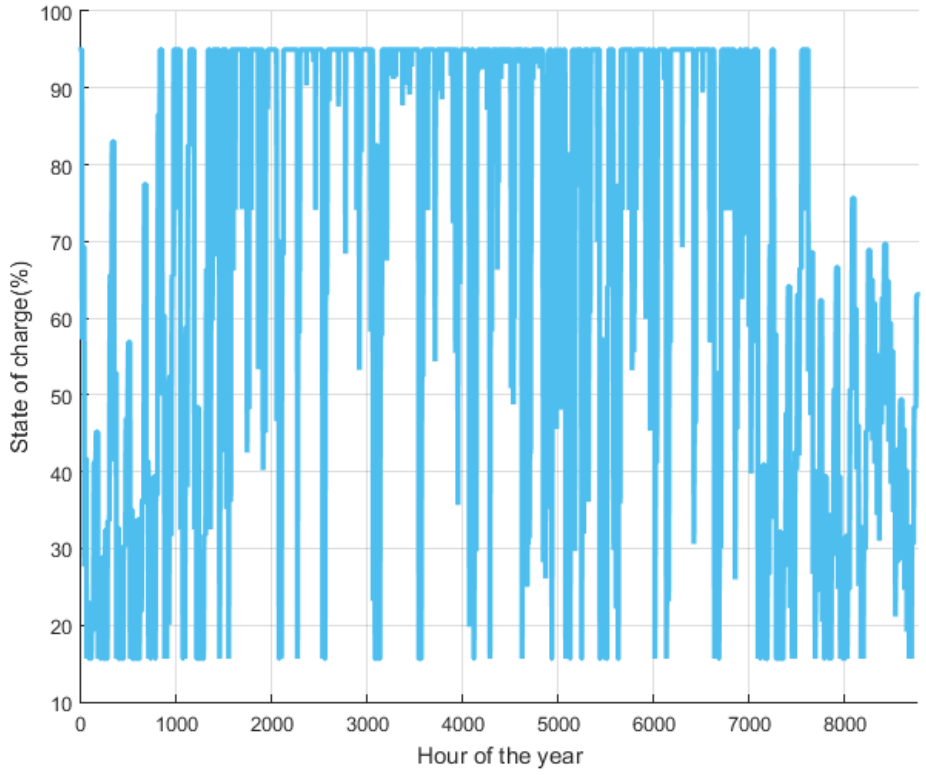


**Figure 82 State of charge of the lithium-iron batteries – Full Model**

In Table 27, some values that represent the interaction with the grid are shown. The grid concept in this off-grid system is only used to explain that at some points the system will not be able to provide the energy required by the load. This means, if there is no connection to the grid, the window will be opaque instead of transparent. In this table, it can be seen that the percentage of energy required from an external source is 3.09% of the energy required in a year with the control system explained in section 10.2.

**Table 27 Values of grid interaction with the system in a year – Full Model**

| | Values |
|---|---|
| Number of hours the grid provides power to the load in a year (h) | 38 |
| Amount of energy provided by the grid in a year (Wh) | 43.34 |
| Grid hour usage in a year (%) | 0.43 |
| Percentage of the total energy needed provided by the grid (%) | 3.09 |

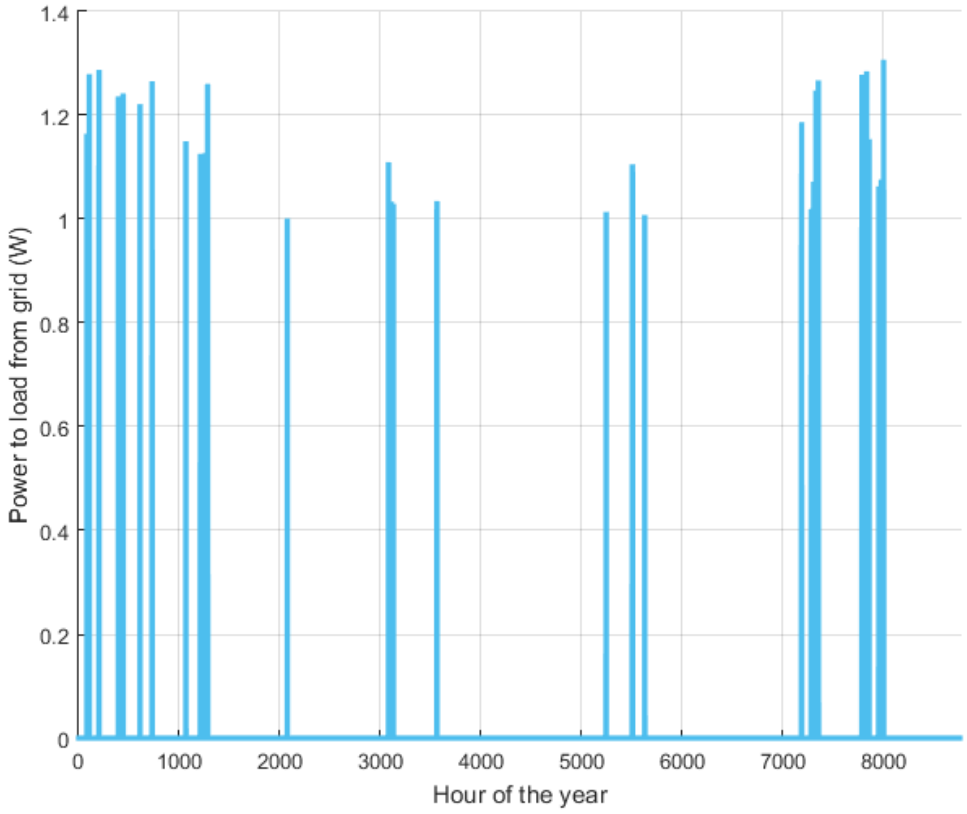


**Figure 83 Power provided by the grid to the load in a year – Full Model**

As it was explained before, in Figure 83 the power supplied by a grid to the load when the full 3D model is used, is shown. This graph will be compared with the other 3 scenarios explained in section 10.2, later in this sub-chapter.

First, the diurnal shading factors for the 4 models (Full Model, A, B and C) are shown in Figure 84, Figure 85, Figure 86 and Figure 87 (respectively). The shading factors express what the shading state of the array is at any time of the day, during every month of the year. In this case only the shading factors from 00:00 to 12:00 are shown, this is because after 12:00 the array is completely shaded until 00:00, where the shading behaviour repeats again. A shading factor of 100, means that the array is completely shaded. Any number below 100 means that there is partial shading over the array, except

0 which means that the array has no shading at that moment of the day. The rows represent each month of the year, starting from January and ending in December.

From the shading factor distribution shown in these figures the first thing that is noticed is that Scenario B and Scenario C have the same distribution even when the 3D model has more shading components for Scenario B than for Scenario C. This behaviour is expected because of the location of the house and the shading components that are removed from Scenario B. For Delft, where the PV array has an azimuth towards the north, the elements that create shade are mostly the ones located at the south. The shading elements removed in Scenario B were all located at the south of the house. In other words, what is really producing shade to the array are the houses and trees removed from the south and not all the buildings. This can be verified with Figure 79 and Figure 80.

| 00:00 | 01:00 | 02:00 | 03:00 | 04:00 | 05:00 | 06:00 | 07:00 | 08:00 | 09:00 | 10:00 | 11:00 | 12:00 |
|---|---|---|---|---|---|---|---|---|---|---|---|---|
| 100 | 100 | 100 | 100 | 100 | 100 | 100 | 100 | 100 | 0 | 0 | 100 | 100 |
| 100 | 100 | 100 | 100 | 100 | 100 | 100 | 100 | 0 | 0 | 0 | 100 | 100 |
| 100 | 100 | 100 | 100 | 100 | 100 | 100 | 0 | 0 | 0 | 0 | 100 | 100 |
| 100 | 100 | 100 | 100 | 100 | 100 | 100 | 21.212 | 0 | 0 | 0 | 100 | 100 |
| 100 | 100 | 100 | 100 | 100 | 100 | 0 | 100 | 0 | 0 | 0 | 100 | 100 |
| 100 | 100 | 100 | 100 | 100 | 100 | 0 | 100 | 0 | 0 | 0 | 0 | 100 |
| 100 | 100 | 100 | 100 | 100 | 100 | 0 | 100 | 100 | 0 | 0 | 0 | 100 |
| 100 | 100 | 100 | 100 | 100 | 100 | 100 | 100 | 0 | 0 | 0 | 100 | 100 |
| 100 | 100 | 100 | 100 | 100 | 100 | 100 | 0 | 0 | 0 | 0 | 100 | 100 |
| 100 | 100 | 100 | 100 | 100 | 100 | 100 | 0 | 0 | 0 | 0 | 100 | 100 |
| 100 | 100 | 100 | 100 | 100 | 100 | 100 | 100 | 0 | 0 | 100 | 100 | 100 |
| 100 | 100 | 100 | 100 | 100 | 100 | 100 | 100 | 100 | 0 | 100 | 100 | 100 |

Figure 84 Shading factors diurnal Full Model

| 00:00 | 01:00 | 02:00 | 03:00 | 04:00 | 05:00 | 06:00 | 07:00 | 08:00 | 09:00 | 10:00 | 11:00 | 12:00 |
|---|---|---|---|---|---|---|---|---|---|---|---|---|
| 100 | 100 | 100 | 100 | 100 | 100 | 100 | 100 | 100 | 0 | 0 | 100 | 100 |
| 100 | 100 | 100 | 100 | 100 | 100 | 100 | 100 | 0 | 0 | 0 | 100 | 100 |
| 100 | 100 | 100 | 100 | 100 | 100 | 100 | 0 | 0 | 0 | 0 | 100 | 100 |
| 100 | 100 | 100 | 100 | 100 | 100 | 0 | 0 | 0 | 0 | 0 | 100 | 100 |
| 100 | 100 | 100 | 100 | 100 | 100 | 0 | 0 | 0 | 0 | 0 | 100 | 100 |
| 100 | 100 | 100 | 100 | 100 | 100 | 0 | 0 | 0 | 0 | 0 | 0 | 100 |
| 100 | 100 | 100 | 100 | 100 | 100 | 0 | 0 | 0 | 0 | 0 | 0 | 100 |
| 100 | 100 | 100 | 100 | 100 | 100 | 0 | 0 | 0 | 0 | 0 | 100 | 100 |
| 100 | 100 | 100 | 100 | 100 | 100 | 0 | 0 | 0 | 0 | 0 | 100 | 100 |
| 100 | 100 | 100 | 100 | 100 | 100 | 100 | 0 | 0 | 0 | 0 | 100 | 100 |
| 100 | 100 | 100 | 100 | 100 | 100 | 100 | 100 | 0 | 0 | 100 | 100 | 100 |
| 100 | 100 | 100 | 100 | 100 | 100 | 100 | 100 | 100 | 0 | 100 | 100 | 100 |

Figure 85 Shading factors diurnal Scenario A

| 00:00 | 01:00 | 02:00 | 03:00 | 04:00 | 05:00 | 06:00 | 07:00 | 08:00 | 09:00 | 10:00 | 11:00 | 12:00 |
|---|---|---|---|---|---|---|---|---|---|---|---|---|
| 100 | 100 | 100 | 100 | 100 | 100 | 100 | 100 | 100 | 0 | 0 | 100 | 100 |
| 100 | 100 | 100 | 100 | 100 | 100 | 100 | 100 | 0 | 0 | 0 | 100 | 100 |
| 100 | 100 | 100 | 100 | 100 | 100 | 100 | 0 | 0 | 0 | 0 | 100 | 100 |
| 100 | 100 | 100 | 100 | 100 | 100 | 0 | 0 | 0 | 0 | 0 | 100 | 100 |
| 100 | 100 | 100 | 100 | 100 | 0 | 0 | 0 | 0 | 0 | 0 | 100 | 100 |
| 100 | 100 | 100 | 100 | 0 | 0 | 0 | 0 | 0 | 0 | 0 | 0 | 100 |
| 100 | 100 | 100 | 100 | 100 | 0 | 0 | 0 | 0 | 0 | 0 | 0 | 100 |
| 100 | 100 | 100 | 100 | 100 | 0 | 0 | 0 | 0 | 0 | 0 | 100 | 100 |
| 100 | 100 | 100 | 100 | 100 | 100 | 0 | 0 | 0 | 0 | 0 | 100 | 100 |
| 100 | 100 | 100 | 100 | 100 | 100 | 100 | 0 | 0 | 0 | 0 | 100 | 100 |
| 100 | 100 | 100 | 100 | 100 | 100 | 100 | 100 | 0 | 0 | 100 | 100 | 100 |
| 100 | 100 | 100 | 100 | 100 | 100 | 100 | 100 | 100 | 0 | 100 | 100 | 100 |

Figure 86 Shading factors diurnal Scenario B

| 00:00 | 01:00 | 02:00 | 03:00 | 04:00 | 05:00 | 06:00 | 07:00 | 08:00 | 09:00 | 10:00 | 11:00 | 12:00 |
|---|---|---|---|---|---|---|---|---|---|---|---|---|
| 100 | 100 | 100 | 100 | 100 | 100 | 100 | 100 | 100 | 0 | 0 | 100 | 100 |
| 100 | 100 | 100 | 100 | 100 | 100 | 100 | 100 | 0 | 0 | 0 | 100 | 100 |
| 100 | 100 | 100 | 100 | 100 | 100 | 100 | 0 | 0 | 0 | 0 | 100 | 100 |
| 100 | 100 | 100 | 100 | 100 | 100 | 0 | 0 | 0 | 0 | 0 | 100 | 100 |
| 100 | 100 | 100 | 100 | 100 | 0 | 0 | 0 | 0 | 0 | 0 | 100 | 100 |
| 100 | 100 | 100 | 100 | 0 | 0 | 0 | 0 | 0 | 0 | 0 | 0 | 100 |
| 100 | 100 | 100 | 100 | 100 | 0 | 0 | 0 | 0 | 0 | 0 | 0 | 100 |
| 100 | 100 | 100 | 100 | 100 | 0 | 0 | 0 | 0 | 0 | 0 | 100 | 100 |
| 100 | 100 | 100 | 100 | 100 | 0 | 0 | 0 | 0 | 0 | 0 | 100 | 100 |
| 100 | 100 | 100 | 100 | 100 | 100 | 0 | 0 | 0 | 0 | 0 | 100 | 100 |
| 100 | 100 | 100 | 100 | 100 | 100 | 100 | 0 | 0 | 0 | 0 | 100 | 100 |
| 100 | 100 | 100 | 100 | 100 | 100 | 100 | 100 | 0 | 0 | 100 | 100 | 100 |
| 100 | 100 | 100 | 100 | 100 | 100 | 100 | 100 | 100 | 0 | 100 | 100 | 100 |

Figure 87 Shading factors diurnal Scenario C

The next variable that will be discussed is the interaction with the grid that changes with the different shading scenarios presented. The 3 cases are shown in Table 28, Table 29 and Table 30.

In first place, Scenario B requires 28 hours of grid energy in a year whereas Scenario C requires 21. These 2 scenarios, compared to the hours required in the Full Model, require 26.32% and 44.74% less hours, respectively. These percentages reflect the sensitivity of the array to shading. In the case of Scenario A the number of hours is reduced to 33, compared to the full model and it represents 13.16% less hours. The location of the array is then an important variable. The location also includes the azimuth of the PV array.

**Table 28 Values of grid interaction with the system in a year – Scenario A**

| | Values |
|---|---|
| Number of hours the grid provides power to the load in a year (h) | 33 |
| Amount of energy provided by the grid in a year (Wh) | 37.81 |
| Grid hour usage in a year (%) | 0.38 |
| Percentage of the total energy needed provided by the grid (%) | 2.69 |

**Table 29 Values of grid interaction with the system in a year – Scenario B**

| | Values |
|---|---|
| Number of hours the grid provides power to the load in a year (h) | 28 |
| Amount of energy provided by the grid in a year (Wh) | 32.27 |
| Grid hour usage in a year (%) | 0.32 |
| Percentage of the total energy needed provided by the grid (%) | 2.30 |

**Table 30 Values of grid interaction with the system in a year – Scenario C**

| | Values |
|---|---|
| Number of hours the grid provides power to the load in a year (h) | 21 |
| Amount of energy provided by the grid in a year (Wh) | 24.71 |
| Grid hour usage in a year (%) | 0.24 |
| Percentage of the total energy needed provided by the grid (%) | 1.76 |

The energy provided by the grid also changes, this is directly related with the number of hours that the grid needs to supply to the system. As expected, and shown in Table 28, Table 29 and Table 30, the percentage of total energy provided by the grid decreases from Scenario A to Scenario C. The comparison between the Full Model and Scenario C, shows that the energy needed is reduced to almost half from one to the other.

This values are supported with Figure 88. In this figure the evolution of the power supplied by the grid to the load in the 3 Scenarios is shown. As it can be seen in each case there is a reduction of peaks, each peak represents an hour. The main hours where the grid needs to supply to the system are located in the winter months, this is an expected behaviour. The irradiance in this months is the lowest of the year in Delft.

Even though there is a need of energy from the grid, there is also a supply from the system to the grid through the year. This supply could exist if the system was connected to the grid, which in this case is not desired but it could be considered in future works. This energy could be also stored and used in other smart windows in the building. This supply to the grid, is due to the control system imposed, where not every hour in the day the PDLC is consuming energy. The energy supplied from the array to the grid is shown in Figure 89 for the 3 shading scenarios.

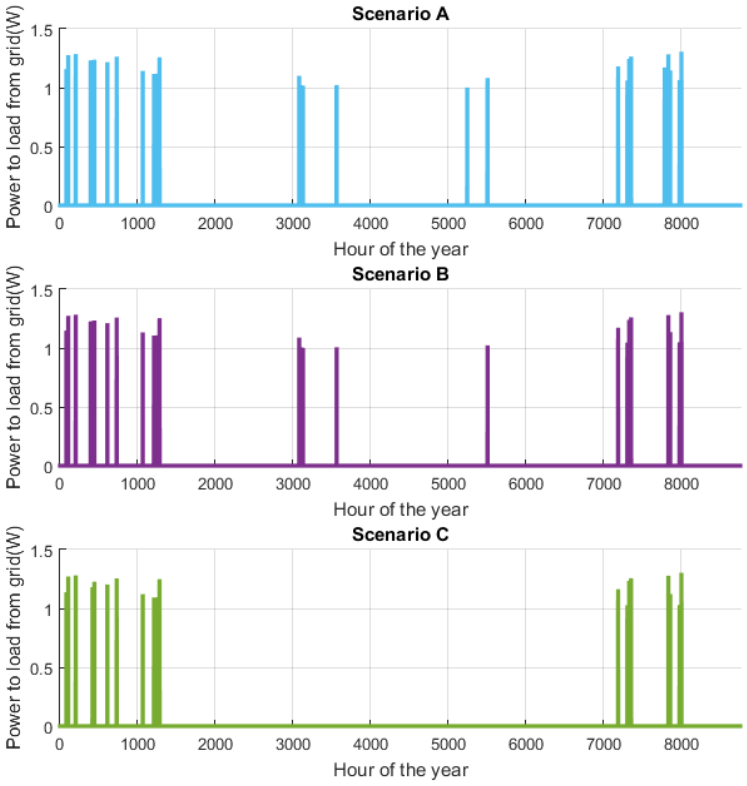


Figure 88 Power to load from grid for Scenario A, B and C, respectively.

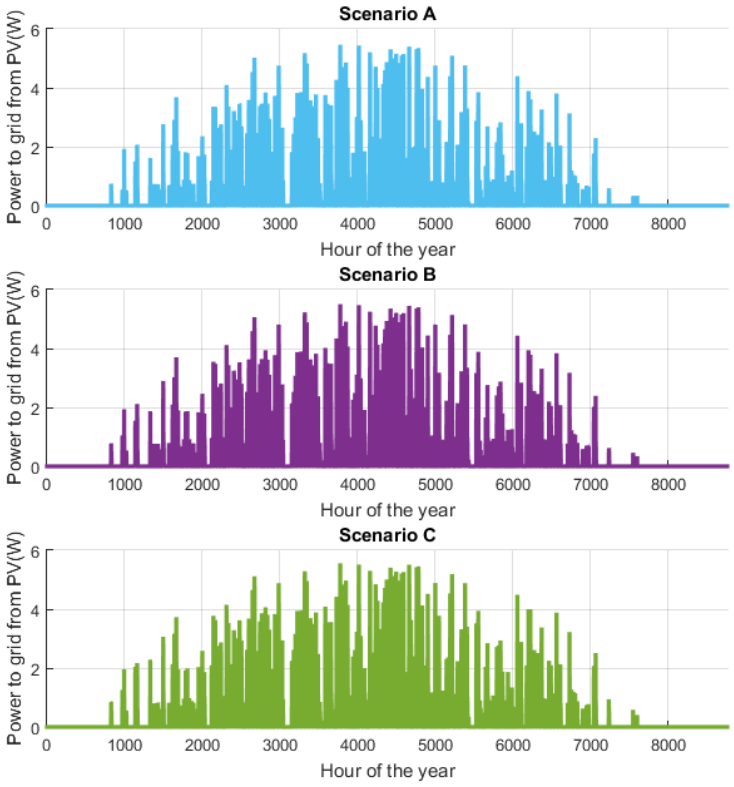


Figure 89 Power to grid from PV for Scenario A, B and C, respectively.

# 11 Conclusions

After the project was developed and the milestones proposed for it were achieved, the conclusions about the prototype, the idea and the complete process were drawn and are presented below.

To begin with, the advantages of the PDLC over the other two electrically actuated glazing technologies will be explained. The PDLC has a shorter time response than the EC film. Even though the PDLC has around the same time response of the SPD, the market status of the first one is better. This technology is currently being researched and it is growing in the market, which makes it a cheaper and more accessible material. Another advantage is that the PDLC has the best transmittance in transparent state from all the films presented, this is a very important parameter because it is the closest behaviour to the traditional transparent glazing used in buildings. A higher direct transmittance means that the natural light requirements and the comfort of the users will be better satisfied. Moreover, choosing the PDLC is also a more appealing research decision than the EC because it involves the conversion of direct current (DC) to alternative current (AC) which is needed to actuate the film. Finally, there is no need to treat the surface of the material, the PDLC has a wide view angle and because it needs a constant power source different levels of opacity can be achieved by tuning the voltage [26].

The energy requirement for the implementation of a PDLC film in the built environment depends on the AC voltage required by the film, and this varies depending on the manufacturer and the size of it. For this particular project, a 48 V PDLC film from Innoglass was selected and the power requirement is 3.7 $\frac{W}{m^2}$. This means that in a year, for 1 $m^2$ of film, the energy requirement is 32.41 kWh. For this case, where the size is 0.36 $m^2$, the yearly energy requirement is 11.67 kWh.

To build a prototype and see how this type of technology can be coupled with PV technology, a 60 x 60 cm glazing size was chosen. This size was restricted by the laminator size available in the PVMD department. The way to couple the PDLC film with any PV technology (cell, module) in an off-grid type of system, is by incorporating a balance of system that contains an MPPT, a charge controller, batteries and most importantly an inverter. All of these elements are necessary for the PDLC to work with the PV array. After the prototype was built, it was tested and it was proven that the two technologies can be coupled together.

To test the feasibility of the product in a real life scenario, a shop in Delft is modelled in the software SAM. The shop's window has an orientation of 58.74°, taking north as 0°. This orientation will correspond to the azimuth of the module too, because it is located exactly on the surface of the glazing. For the model, a control decision based on direct beam irradiance and temperature is made so that the glazing is transparent and opaque in different times of the day throughout the whole year. After the loading conditions were input in SAM, the model was run and the results show a 3.09% time dependency of the product to the grid. To test the shading sensitivity of the PDLC + PV system, 3 scenarios where made using the full model as a base. The results of the scenarios showed that the grid time dependency can be reduced to 1.76% when there are no shading elements around the building where the smart window is located.

# 12 Future Work

In the final chapter of this project, the recommendations and future work that needs to be done in order to assess the feasibility of this product from an architectural point of view will be introduced. The importance of assuring user comfort and safety is a requirement for every product that will eventually reach the market. This has to be done in future projects. Furthermore, different control decisions can be made to assess the PV + PDLC system and different scenarios and locations can also be selected.

## 12.1. Smart Window Characterization

The feasibility of the technical aspects of the window were assessed along this project. However, for this system to reach the market, other important aspects have to be considered. Glazing is a crucial part of building façade and it is the layer were natural daylight can come in, either in the form of light or in the form of heat. Although natural light is very important for human comfort some sections of its spectrum are dangerous for health and material lifetime.

The first two variables that should be calculated are the Solar Skin Protection Factor and the Solar Material Protection Factor. These two factors “indicate how well the glazing material can protect the human skin and building material behind the glazing from solar radiation [55].” These factors have a range from 0 to 1 and the closer the values are to 1, the higher the protection the glazing provides. To calculate these factors, the spectral transmission of the glazing and the relative spectral distribution of solar radiation have to be obtained.

The next two variables needed are the Colour-Rendering Index (CRI) and the Correlated Colour Temperature (CCT). These two colour properties are used to assess the quality of daylight that enters through the glazing. CRI goes in a scale of 0 to 100 and the closest the value is to 100, the better the visual quality. Visual quality refers to “no significant perceived colour difference between objects illuminated by daylight and by the same illuminant transmitted through a glazing [56].” CCT is a temperature value, as the name indicates. CCT of the sky can vary between 6000 K and 10000 K [56].

Finally, the two most used variables that should be characterized for this PV + PDLC system are the g-value and the u-value. The g-value is also known as the Solar Heat Gain Coefficient, which has been mentioned before in this report. It “indicates the transmitted solar energy through a glazing [55].” The transmitted solar energy is the sum of the transmittance and the infrared radiation that crosses the glazing [55]. The u-value is a more complex variable. It refers to the conductivity of the window. The formal definition is “a measure of the heat transmission through a building part (such as a wall or window) or a given thickness of a material (such as insulation) with lower numbers indicating better insulating properties [57].” It is used to indicate how good is the façade element in keeping the heat inside the structure in the winter and rejecting it during the hottest months.

## 12.2. Other Recommendations

As it was said before, it is recommended to do a better control decision for the system. The reason for this is to represent, with more accuracy, the working load of the PV system attached to the glazing. It is also recommended to implement the control algorithm and try it with physical prototypes in order to ensure that the PDLC is able to meet this control demands.

Another important research that can be done is the design of the PV + PDLC system to be implemented in a whole building. During the project it was thought of the feasibility of the product when more than one window is considered. It will be good to understand how the balance of system will change in order to supply to several smart windows at the same time. As a starting point a central inverter with optimizers attached to each PV + PDLC system could be a solution. Each side and each floor of the building could be seen as a string of PV arrays. With each window having its own optimizer, the voltage supply, which is the most important variable for the PDLC state, can be guaranteed more often. Furthermore, each side of the building can contribute to a single storage system, which will reduce the impact of shading in the energy harvest. This last statement compared to each side having its own storage system. Having a central inverter is feasible in this case, because the PDLC has a nominal fixed voltage to change its state. If every glazing of the building is designed with the same PDLC technology the output of the inverter(s) can be the same.

Of course if a more sophisticated control decision is done, i.e. that the transparency of each window is adjusted between a voltage range, more complex solutions have to be implemented. These solutions depend on the voltage output of the inverter(s) and it will have to be different for every smart window in the building.

# Bibliography


[1] United Nations Framework Convention on Climate Change, “Paris Agreement,” United Nations, Paris, 2015.

[2] Solar Power Europe, “Global Market Outlook,” Brussels, 2018.

[3] UN Environment and International Energy Agency , “Towards a zero-emission, efficient, and resilient buildings and construction sector. Global Status Report 2017.,” 2017.

[4] Orbis Research, “Global Construction Market Outlook to 2022,” 12 March 2019. [Online]. Available: https://www.reuters.com/brandfeatures/venture-capital/article?id=90251. [Accessed 20 Aug 2019].

[5] CHPS, “Daylighting and Fenestration Design,” 2002. [Online]. Available: https://www.lightingassociates.org/i/u/2127806/f/tech_sheets/daylighting_and_fenestration_design.pdf. [Accessed 18 04 2019].

[6] A. Ghosh and B. Norton, “Advances in switchable and highly insulating autonomous (self-powered) glazing systems for adaptive low energy buildings,” *Renewable Energy,* vol. 126, pp. 1003-1031, 2018.

[7] T. Bartuska and G. Young, “The Built Environment Definition and Scope,” in *The Built Environment: A Creative Inquiry into Design and Planning*, Crisp Publications, Inc, 1994, pp. 3-13.

[8] University of Alberta, “What is sustainability?,” 27 06 2013. [Online]. Available: https://www.mcgill.ca/sustainability/files/sustainability/what-is-sustainability.pdf. [Accessed 02 2019].

[9] J. Sarkis, L. Meade and A. Presley, “Sustainability in the built environment: factors and a decision framework,” in *Handbook of Corporate Sustainability: Frameworks, Strategies and Tools.*, Cheltenham, MPG Books Group UK, 2009, pp. 2581-2586.

[10] A. F. M. a. P. D. Schneider, “ A new map of global urban extent from MODIS satellite data,” *Environmental Research Letters,* vol. 4, p. 11, 2009.

[11] R. Laing, “Towards More Sustainable Built,” in *Innovations for Sustainable Building Design and Refurbishment in Scotland, Green Energy and Technology*, Glasgow, Springer International Publishing Switzerland, 2013, pp. 11-17.

[12] Building Performance Institute Europe, “Nearly Zero Energy Buildings definition across Europe,” Brussels, 2015.

[13] A. A. Abdoli and H. J. Bakhsh, “Strategies and Techniques for Optimized Design of Façade in High-rise Buildings: An Energy-Efficient Approach: A Case Study in a Residential Tower Located in Urban District 22, Tehran, Iran,” *European Online Journal of Natural and Social Sciences,* vol. 3, no. 4, pp. 228-237, 2014.

[14] H. M. Sacht, L. Braganca and M. Almeida, “Repositorium University of Minho,” 24 09 2010. [Online]. Available:

https://repositorium.sdum.uminho.pt/bitstream/1822/14017/1/Sacht.pdf. [Accessed 02 2019].

[15] T. Ihara, A. Gustavsen and B. P. Jelle, “Effect of facade components on energy efficiency in office buildings,” *Applied Energy,* vol. 158, pp. 422-432, 2015.

[16] M. Sabry, P. Eames, H. Singh and Y. Wue, “Smart windows: Thermal modelling and evaluation,” *Solar Energy,* vol. 103, pp. 200-209, 2014.

[17] C. M. Lampert, “Large-area smart glass and integrated photovoltaics,” *Solar energy materials and solar cells,* vol. 76, no. 4, p. 76, 2003.

[18] MSE Supplies, “GLOBAL SMART GLASS MARKET TO GROW TO $5.8 BILLION USD BY 2020,” 22 Jan 2016. [Online]. Available: https://www.msesupplies.com/blogs/news/34196932-global-smart-glass-market-to-grow-to-5-8-billion-usd-by-2020. [Accessed 11 July 2019].

[19] M. Casini, “Active dynamic windows for buildings: A review,” *Renewable Energy,* vol. 119, pp. 923-934, 2018.

[20] H. Hakemi, “Polymer-dispersed liquid crystal technology ‘industrial evolution and current market situation’,” *Liquid Crystals Today,* vol. 26, no. 3, pp. 70-73, 2017.

[21] Y. Lin, H. Ren and S. Wu, “Polarisation-independent liquid crystal devices,” *Liquid Crystals Today,* vol. 17, no. 1-2, pp. 2-8, 2008.

[22] D. Cupelli, F. P. Nicoletta, S. Manfredi, M. Vivacqua, P. Formoso, G. D. Filpo and G. Chidichimo, “Self-adjusting smart windows based on polymer-dispersed liquid crystals,” *Solar energy materials and solar cells,* vol. 93, pp. 2008-2012, 2009.

[23] S. K. &. V. Z. Sergei Bronnikov, “Polymer-Dispersed Liquid Crystals: Progress in Preparation, Investigation, and Application.,” *Journal of Macromolecular Science,* vol. 52, no. 12, pp. 1718-1735, 2013.

[24] B. G. A. &. M. T. Norton, “Daylight Characteristics of a Polymer Dispersed Liquid Crystal Switchable Glazing,” *Solar Energy Materials and Solar Cells,* vol. 174, pp. 572-576, 2018.

[25] D. Jung, W. Choi, J.-Y. Park, K. B. Kim, N. Lee, Y. Seo, H. S. Kim and N. K. Kong, “Inorganic gel and liquid crystal based smart window using silica sol-gel process,” *Solar energy materials and solar cells,* vol. 159, pp. 488-495, 2017.

[26] D.-J. Kim, D. Y. Hwang, J.-Y. Park and H.-K. Kim, “Liquid crystal-based flexible smart windows on roll-to-roll slot die-coated Ag nanowire network films,” *Journal of alloys and compounds,* vol. 765, pp. 1090-1098, 2018.

[27] H. Hakemi, “Industrial Development of Plastic PDLC: Is There a Future?,” *Liquid Crystals Today,* vol. 8, no. 3, pp. 7-12, 1998.

[28] S.-W. Oh, J.-M. Baek and T.-H. Yoon, “Sunlight-switchable light shutter fabricated using liquid crystals doped with push-pull azobenzene,” *Optics Express,* vol. 24, no. 23, pp. 26575-26582, 2016.

[29] S. Glunz, R. Preu and D. Biro, “Crystalline Silicon Solar Cells: State-of-the-Art and Future Developments,” *Comprehensive Renewable Energy,* vol. 1, pp. 353-387, 2012.

[30] A. Smets, K. Jäger, O. Isabella, R. V. Swaaij and M. Zeman, Solar Energy: the physics and engineering of photovoltaic conversion thecnologies and systems, Cambridge: UIT Cambridge, 2016.

[31] AKW, *MONO 3BB 5.0W 100PC,* 2019.

[32] Sunpower, “MAXEON GEN III SOLAR CELLS,” 20 Dic 2017. [Online]. Available: https://us.sunpower.com/sites/sunpower/files/media-library/spec-sheets/sp-sunpower-maxeon-solar-cells-gen3.pdf. [Accessed 1 Mar 2019].

[33] Sunpower, “Sunpower Solar Cell Technology,” 2019. [Online]. Available: https://us.sunpower.com/why-sunpower/maxeon-solar-cells. [Accessed 12 July 2019].

[34] Innoglass, “Switchable PDLC Film Specification,” www.inno-glass.com, Qingdao, 2018.

[35] Pro-lite technology, “Spectralon Reflectance Material,” [Online]. Available: https://www.pro-lite.co.uk/File/spectralon_material.php. [Accessed 05 May 2019].

[36] Perkin Elmer, “LAMBDA 950 UV/Vis Spectrophotomete,” 2019. [Online]. Available: https://www.perkinelmer.com/es/product/lambda-950-uv-vis-nir-spectrophotometer-l950. [Accessed 5 July 2019].

[37] WACOM, “LED Solar simulator,” [Online]. Available: http://www.wacom-ele.co.jp/en/products/solar/led/. [Accessed 23 04 2019].

[38] TU DELFT-PVMD, “Task 3. Photovoltaic Modules,” Delft, 2017-2018.

[39] Y. Gao, “Photovoltaic Windows: theories, devices and applications,” repository.tudelft.nl, Delft, 2019.

[40] Smart Tint, “ST1230-75PM DC-Smart Tint Mobile Module Adapter,” 2019. [Online]. Available: https://shop.smarttint.com/ST1230-75PM-DC-Smart-Tint-Mobile-Module-Adapter_p_3256.html. [Accessed 17 Abril 2019].

[41] Ali Express, “6S/7S Lithium 8S Lithium Iron Phosphate 18V Boost MPPT Battery Charger Boar Module Solar controller CN3306,” 2019. [Online]. Available: https://nl.aliexpress.com/. [Accessed 2 June 2019].

[42] Consonance, “Step-up Multi-Chemistry Battery Charger IC with PhotoVoltaic Cell MPPT Function,” 20 Feb 2019. [Online]. Available: http://www.consonance-elec.com/pdf/datasheet/DSE-CN3306.pdf. [Accessed 2 July 2019].

[43] Y. Verbelen, “Characterization of Self-Powered Autonomous Embedded Systems for Complementary Balanced Energy Harvesting,” University of Bristol, Bristol, 2018.

[44] Z Battery, “LiFePO4 3.2V 400 mah 4/5 AA Rechargeable 14430 Battery, LFP-14430-400A,” [Online]. Available: https://zbattery.com/LiFePO4-3-2V-4-5-AA-Rechargeable-14430-Battery. [Accessed 7 July 2019].

[45] S. J. A. A.-O. T. S. John D’Orazio, “UV Radiation and the Skin,” *International Journal of Molecular Sciences,* vol. 14, no. 6, pp. 12222-12248, 2013.

[46] Hunter Lab Sverige, “Applications Note,” 4 June 2008. [Online]. Available: https://www.hunterlab.se/wp-content/uploads/2012/11/Haze.pdf. [Accessed 9 July 2019].

[47] STR Holdings, “Photocap,” 16 Jan 2015. [Online]. Available: http://www.strsolar.com/UploadedFiles/Files/15580P_2015-01.pdf. [Accessed 28 Feb 2019].

[48] E. Hahne and R. Pfluger, “Improvements on PASSYS Test Cells,” *Solar Energy,* vol. 58, no. 4, pp. 239-246, 1996.

[49] PVMD TU Delft, “Public PVMD monitoring dashboard,” [Online]. Available: https://www.pvmonitoring.pvmd.tudelft.nl/. [Accessed 5 Aug 2019].

[50] NREL, “System Advisor Model (SAM),” 2019. [Online]. Available: https://sam.nrel.gov/. [Accessed 19 July 2019].

[51] Meteotest, “Meteonorm,” 3 Dec 2018. [Online]. Available: https://meteonorm.com/. [Accessed June 2019].

[52] Google, “Google Maps,” 2019. [Online]. Available: https://www.google.com/maps. [Accessed 15 June 2019].

[53] H. T. Remøy, Out of Office: A Study on the Cause of Office Vacancy and Transformation as a Means to Cope and Prevent, Heroy: Norwegian University of Science and Technology, 2010.

[54] NREL, “SAM Photovoltaic Model Technical Reference,” May 2015. [Online]. Available: https://www.nrel.gov/docs/fy15osti/64102.pdf. [Accessed 20 July 2019].

[55] M. T. Ghosh A., “Evaluation of optical properties and protection factors of a PDLC switchable glazing for low energy building integration,” *Solar Energy Materials and Solar Cells,* vol. 176, pp. 391-396, 2018.

[56] M. T. Ghosh A., “Evaluation of colour properties due to switching behaviour of a PDLC glazing for adaptive building integration,” *Renewable Energy,* vol. 120, pp. 126-133, 2018.

[57] Merriam-Webster Dictionary, 2019. [Online]. Available: https://www.merriam-webster.com/dictionary/U-value. [Accessed 18 Aug 2019].